SCIENTIFIC REPORTS

OPEN

Received: 12 August 2016
Accepted: 23 January 2017
Published: 24 February 2017

Caulobacter crescentus CdnL is a non-essential RNA polymerase-binding protein whose depletion impairs normal growth and rRNA transcription

Aránzazu Gallego-García[1], Antonio A. Iniesta[1], Diego González[2,†], Justine Collier[2], S. Padmanabhan[3] & Montserrat Elías-Arnanz[1]

CdnL is an essential RNA polymerase (RNAP)-binding activator of rRNA transcription in mycobacteria and myxobacteria but reportedly not in *Bacillus*. Whether its function and mode of action are conserved in other bacteria thus remains unclear. Because virtually all alphaproteobacteria have a CdnL homolog and none of these have been characterized, we studied the homolog ($CdnL_{Cc}$) of the model alphaproteobacterium *Caulobacter crescentus*. We show that $CdnL_{Cc}$ is not essential for viability but that its absence or depletion causes slow growth and cell filamentation. $CdnL_{Cc}$ is degraded *in vivo* in a manner dependent on its C-terminus, yet excess $CdnL_{Cc}$ resulting from its stabilization did not adversely affect growth. We find that $CdnL_{Cc}$ interacts with itself and with the RNAP β subunit, and localizes to at least one rRNA promoter *in vivo*, whose activity diminishes upon depletion of $CdnL_{Cc}$. Interestingly, cells expressing $CdnL_{Cc}$ mutants unable to interact with the RNAP were cold-sensitive, suggesting that $CdnL_{Cc}$ interaction with RNAP is especially required at lower than standard growth temperatures in *C. crescentus*. Our study indicates that despite limited sequence similarities and regulatory differences compared to its myco/myxobacterial homologs, $CdnL_{Cc}$ may share similar biological functions, since it affects rRNA synthesis, probably by stabilizing open promoter-RNAP complexes.

Bacteria adapt to changing conditions by controlling gene expression, and transcription initiation is the most frequently regulated step. Bacterial transcription begins when the RNA polymerase (RNAP) holoenzyme, consisting of the core ($\alpha_2\beta\beta'\omega$) and a specific dissociable σ factor, recognizes a target promoter to form a closed complex (RP_c), which undergoes a series of conformational changes leading to open complex (RP_o) formation and RNA synthesis from the DNA template[1–3]. Defined promoter elements and the choice of a given σ factor are fundamental determinants of target specificity. Nonetheless, numerous accessory factors often play key roles in modulating, positively or negatively, the various steps of transcription initiation.

An emerging class of bacterial RNAP-interacting transcriptional factors are members of the CarD-CdnL family. The global transcriptional regulator CarD, composed of an N-terminal RNAP-interacting domain and a DNA-binding domain resembling eukaryotic HMGA proteins, is found only in myxobacteria, where it is dispensable for cell viability, and has been linked to the action of the alternative extracytoplasmic function (ECF) σ factors[4–7]. By contrast, CdnL (for CarD N-terminal like) is a standalone version of the N-terminal domain of CarD, whose homologs (sometimes referred to as CarD) occur in several bacterial taxonomical groups[5,8–10]. CdnL from *M. xanthus* ($CdnL_{Mx}$) and its *Mycobacterium tuberculosis* homolog ($CdnL_{Mt}$) are essential for cell viability[9,10], as may also be the case for the homolog in the spirochaete *Borrelia burgdorferi*[11]. On the other hand,

[1]Departamento de Genética y Microbiología, Área de Genética (Unidad Asociada al IQFR-CSIC), Facultad de Biología, Universidad de Murcia, 30100 Murcia, Spain. [2]Department of Fundamental Microbiology, Faculty of Biology and Medicine, University of Lausanne, Quartier UNIL/Sorge, Lausanne, CH1015, Switzerland. [3]Instituto de Química Física 'Rocasolano', Consejo Superior de Investigaciones Científicas (IQFR-CSIC), Serrano 119, 28006 Madrid, Spain. [†]Present address: Department of Zoology, University of Oxford, OX1 3PS Oxford, United Kingdom. Correspondence and requests for materials should be addressed to M.E.-A. (email: melias@um.es)

CdnL is reportedly not essential in *Bacillus subtilis*[12,13] or in *Bacillus cereus*[14], suggesting that its function is not always conserved. In fact, many members of the phylum Firmicutes, to which *B. subtilis* and *B. cereus* belong, lack a CdnL homolog.

The critical function of CdnL is likely related to its role in promoting gene expression by stabilizing RP_o formation at promoters, such as those for rRNA, that depend on the primary σ factor[15–19]. Like the CarD N-terminal domain, $CdnL_{Mx}$ interacts with the RNAP β subunit (RNAPβ) but, while this interaction is dispensable for CarD, it is crucial for $CdnL_{Mx}$[16,20]. The CdnL-RNAPβ interaction has also been demonstrated for $CdnL_{Mt}$[21], $CdnL_{Tt}$ in *Thermus thermophilus*[10,22], $CdnL_{Bb}$ in *Bdellovibrio bacteriovorus* (a deltaproteobacterium like *M. xanthus*), $CdnL_{Cg}$ in *Corynebacterium glutamicum* and $CdnL_{Sc}$ in *Streptomyces coelicolor*, both actinobacteria like *M. tuberculosis*[16]. The *B. subtilis* homolog $CdnL_{Bs}$ (also named YdeB), however, does not appear to interact with RNAPβ[13].

To establish if CdnL has conserved functions, and to gain insights into structure-function relationships in this large family of proteins, it is imperative to characterize CdnL from diverse classes of bacteria. *Caulobacter crescentus*, a Gram-negative oligotrophic fresh water alphaproteobacterium, is an important model system for studies on bacterial cell cycle, division and differentiation[23]. The alphaproteobacteria class includes members with very varied lifestyles and, although most of them have a CdnL homolog, none had been specifically studied. This prompted us to characterize the homolog in *C. crescentus,* $CdnL_{Cc}$ (26–34% identical to homologs studied in other bacterial species; Supplementary Table S1, Supplementary Fig. S1). Our findings indicate that $CdnL_{Cc}$ is required for normal growth in *C. crescentus* but is not essential for viability, in contrast to $CdnL_{Mt}$ and $CdnL_{Mx}$. Our data show that $CdnL_{Cc}$ is degraded *in vivo* and that this depends on its C-terminal AA motif, although stabilizing $CdnL_{Cc}$ had no apparent effect on growth. We also show that $CdnL_{Cc}$ binds to RNAPβ and localizes to at least one rRNA promoter *in vivo*, whose activity diminishes on limiting intracellular $CdnL_{Cc}$ levels. Given these parallels with $CdnL_{Mx}$, $CdnL_{Mt}$, and $CdnL_{Tt}$, we propose that $CdnL_{Cc}$ may also stabilize open rRNA promoter-RNAP complexes. Interestingly, we find that missense mutations of conserved residues of $CdnL_{Cc}$ that impair the interaction with RNAPβ lead to a cold-sensitive *in vivo* phenotype, suggesting that $CdnL_{Cc}$ interaction with RNAP is functionally more important at lower temperatures in *C. crescentus*. Our results extend the requirement of CdnL for normal cell growth and its possible functional roles in alphaproteobacteria and contribute to elucidating structure-function relationships underlying its mode of action.

Results

CdnL is widespread and highly conserved in alphaproteobacteria. A CdnL homolog was found in all representative alphaproteobacteria, except for the early diverging genus *Magnetococcus*, a clade of Rickettsiales comprising the genera *Neorickettsia*, *Wolbachia*, *Ehrlichia* and *Anaplasma*, and a single Rhodospirillales (*Thalassobaculum_L2*). A phylogenetic tree of these proteins (Supplementary Fig. S2) is globally consistent with the accepted phylogeny of alphaproteobacteria[24], suggesting that CdnL has mostly been transmitted vertically along the phylogeny without long-range lateral gene transfer. Given that other classes of proteobacteria have a CdnL homolog, the most parsimonious hypothesis is that the common ancestor of alphaproteobacteria had a CdnL homolog that was lost along one of the main branches in the Rickettsiales group and, independently, in *Magnetococcus*. The presence of CdnL in most alphaproteobacteria, with high overall amino acid sequence conservation (>50% identity and >90% coverage relative to $CdnL_{Cc}$) suggests strong purifying selection and an important cellular function. Studies with $CdnL_{Cc}$ could thus help understand its role not only in *C. crescentus* but also in other alphaproteobacteria.

$CdnL_{Cc}$ is not essential for viability but is required for normal cell growth. A recent global transcriptional start site (TSS) mapping study in *C. crescentus*[25] listed a single TSS for $cdnL_{Cc}$ and assigned a putative −35 to −10 promoter segment (TTCATAG-x_{12}-GCTATTGT, where x is A, T, C, or G) similar to the consensus for promoters dependent on σ^{73}, the primary σ factor in *C. crescentus* (5′-TTGaCg(c/g)-$x_{11\text{-}14}$-GCtAxA(a/t)C-3′[26,27]). We found that a reporter *lacZ* fusion to the 352-bp intergenic region upstream of $cdnL_{Cc}$, which includes the predicted σ^{73}-dependent promoter, showed high and increasing reporter β-galactosidase activity during exponential growth that leveled off in stationary phase (Supplementary Fig. S3). Interestingly and notably different from $cdnL_{Mx}$ and $cdnL_{Mt}$, the mapped $cdnL_{Cc}$ TSS suggests a long (233 nt) 5′untranslated region (5′-UTR), comparable to the 266-nt one reported for the alphaproteobacterium *Sinorhizobium meliloti* in another global TSS study[28].

A genome-wide transposon insertion analysis suggested that $cdnL_{Cc}$ is essential, or at least has a strong fitness impact, when *C. crescentus* is cultivated in rich medium[29]. Similar studies in other alphaproteobacteria have also listed *cdnL* as essential in *Brevundimonas subvibrioides* (Caulobacterales, like *C. crescentus*)[30] and *Rhodopseudomonas palustris* (Rhizobiales)[31], but it was unclear in *Agrobacterium tumefaciens*[30] and in *Rhizobium leguminosarum*[32] (both Rhizobiales). We therefore probed the functional importance of $cdnL_{Cc}$ by first attempting to generate a markerless, in-frame $cdnL_{Cc}$ deletion ($\Delta cdnL_{Cc}$) with a two-step allele exchange strategy (see Supplementary Methods). Inability to obtain haploid cells with the $\Delta cdnL_{Cc}$ allele (none out of ∼75 colonies analyzed that grew after two days had the $\Delta cdnL_{Cc}$ allele) hinted that $cdnL_{Cc}$ may be essential for viability. This was further supported by the ability to delete $cdnL_{Cc}$ when a second functional copy, expressed under the control of the vanillate-inducible P_{van} promoter, was supplied at a heterologous chromosomal site: approximately a third of the colonies analyzed after the normal two-day growth now had the $\Delta cdnL_{Cc}$ allele (strain ME4). However, ME4 grew without vanillate in the medium, albeit slower than in the presence of the inducer (doubling time ∼ 140 min versus ∼90 min; Fig. 1a,b), suggesting leaky P_{van} expression in the absence of vanillate or that $cdnL_{Cc}$ is not essential. To resolve this issue, we attempted to replace $cdnL_{Cc}$ by a $\Delta cdnL_{Cc}$::Ω allele (conferring spectinomycin/streptomycin resistance) using the two-step allele exchange strategy in the presence of a complementing plasmid, followed by generalized transduction of the $Spec^R/Strep^R$ Ω cassette into the wild-type strain (see Supplementary Methods). A significant number of $Spec^R/Strep^R$ colonies (30–50) grew ∼4–5 days after transduction, which were confirmed to have the $\Delta cdnL_{Cc}$::Ω allele (strain JC784), suggesting that $CdnL_{Cc}$ is in fact

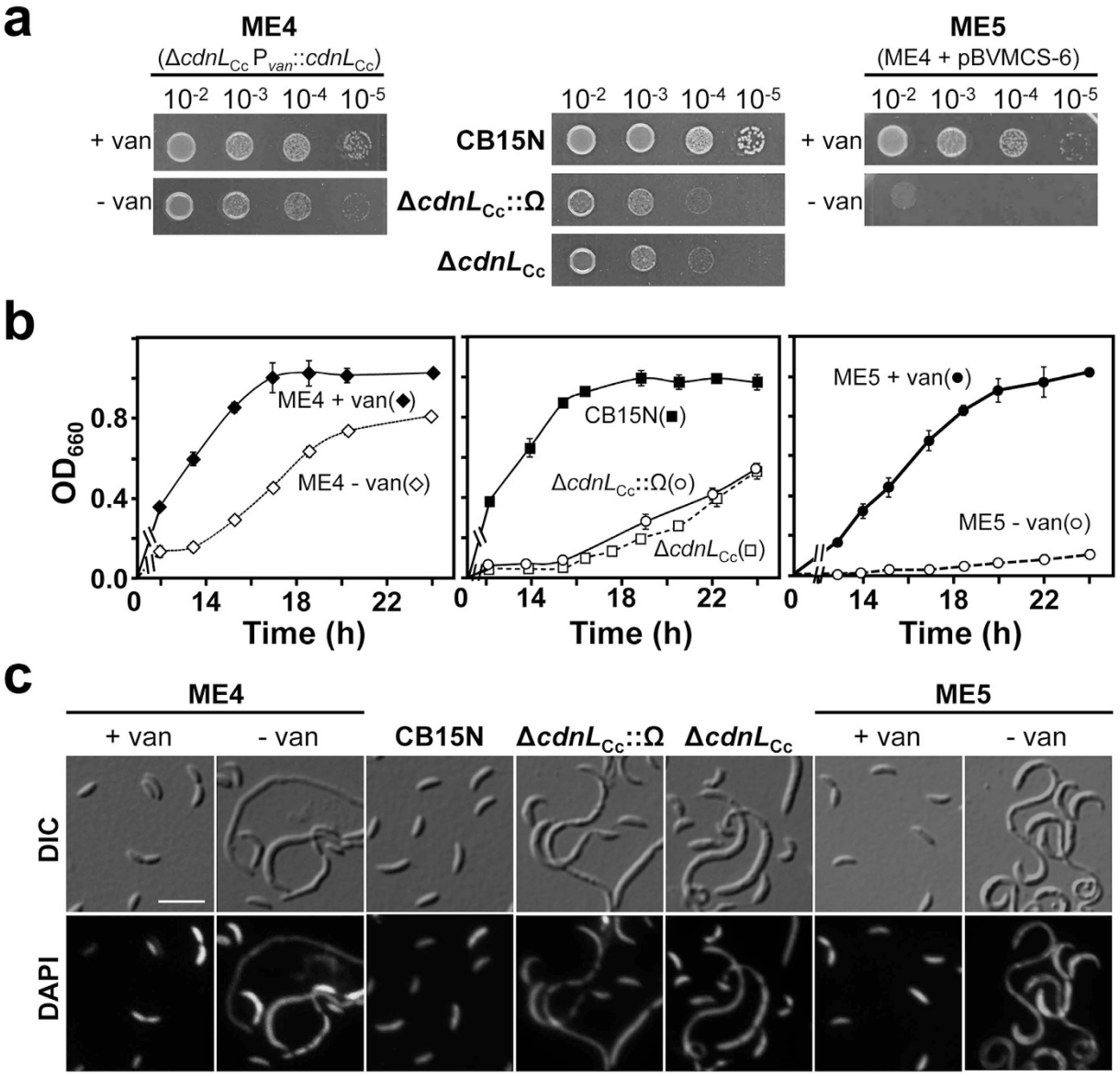

Figure 1. Growth and cell morphology upon CdnL$_{Cc}$ depletion. (**a**) Growth of the indicated *C. crescentus* strains. Liquid cultures (OD$_{660}$ ~ 0.5) were serially diluted, spotted (8 μl) on PYE plates with (+van) or without (−van) 0.5 mM vanillate, and incubated for 2 days at 30 °C. (**b**) Growth curves for the strains indicated (with symbols in parentheses). Freshly plated cells were innoculated into 10 ml of PYE (with 0.5 mM vanillate for ME4 and ME5) and grown at 30 °C to OD$_{660}$ ~ 0.8. 50 μl were aliquoted (for ME4 and ME5, after washing three times with PYE to remove the vanillate) into 10 ml of fresh PYE (for ME4 and ME5, one with 0.5 mM vanillate and one without). Growth was monitored at the indicated times, and the average and error of three independent measurements is shown. (**c**) Cellular morphology of cells from (**b**). Samples (concentrated ten-fold in the case of ME5 cultivated in the absence of vanillate) of each culture in (**b**) after ~20 h of growth were DAPI-stained and examined by DIC (differential interference contrast; top panels) and fluorescence microscopy (bottom panels), as described in Methods. Scale bar: 5 μm.

dispensable but its absence slows down growth (Fig. 1a,b). We therefore repeated our attempt to obtain a markerless Δ*cdnL*$_{Cc}$ strain, plating increasing dilutions to enable detection of slow-growing colonies. Such colonies emerged after ~4–5 days, and all of them had the Δ*cdnL*$_{Cc}$ allele (strain ME50). It is unlikely that these Δ*cdnL*$_{Cc}$ colonies appeared as a consequence of supressor mutations, since they were isolated at a frequency comparable to that observed when a complementing *cdnL*$_{Cc}$ copy was present. Furthermore, both Δ*cdnL*$_{Cc}$ strains (JC784 and ME50), even though generated independently, exhibited the same slow-growth behavior in rich medium (Fig. 1a), with similar doubling times (~230 min; Fig. 1b), which were higher than for the wild type (~90 min) or for ME4 in the absence of vanillate (~140 min). Many JC784 and ME50 cells, and ME4 cells grown in the absence of vanillate, were filamentous indicating cell division defects, and the DNA visualized by DAPI fluorescence was often unevenly distributed (Fig. 1c).

The faster growth rate of ME4 (with no vanillate) relative to JC784 or ME50, suggests leaky P_{van}-$cdnL_{Cc}$ expression. To achieve tighter repression, we introduced a high-copy number plasmid expressing *vanR*, pBVMCS-6[27], into ME4. Growth of the resulting strain (ME5; Fig. 1a–c) in the absence of vanillate was more severely affected than that of ME4 but, curiously, even more so than that of the two Δ$cdnL_{Cc}$ strains (JC784 or ME50). This was also observed when a high-copy number plasmid bearing *vanR* with a different antibiotic resistance marker (pBVMCS-2) was used, or even when such plasmids lacked *vanR* (Supplementary Fig. S4)[27]. Thus, $CdnL_{Cc}$ depletion appears to undermine the ability of cells to cope with the fitness burden due to the presence of these plasmids. The possibility of turning $CdnL_{Cc}$ expression on or off in ME5, together with its more severe growth phenotype upon depleting $CdnL_{Cc}$, led us to use this strain for assessing functionality of $CdnL_{Cc}$ variants in *C. crescentus* (below).

In sum, $CdnL_{Cc}$ is not essential under standard growth conditions on rich medium but its absence or its depletion causes growth and morphological defects, and compromises cell fitness and ability to deal with stresses such as maintaining high-copy number plasmids in *C. crescentus*.

$CdnL_{Cc}$ is degraded *in vivo* in a manner dependent on its C-terminus, but its stabilization does not impair cell growth. $CdnL_{Cc}$ has a C-terminal AA motif (Supplementary Fig. S1), a hallmark of many substrates of the energy-dependent ClpXP protease, essential in *C. crescentus*, where it degrades several proteins implicated in replication, cell cycle or development[33,34]. We therefore examined the stability of $CdnL_{Cc}$ *in vivo*. For this, $CdnL_{Cc}$ was fused to a FLAG epitope tag, to enable detection by immunoblot analysis. Since the tag can mask potential protease recognition, both N- and C-terminally tagged versions were tested. We could generate a normally growing strain expressing the C-terminally FLAG-tagged $CdnL_{Cc}$ ($CdnL_{Cc}$-FLAG) as the sole $CdnL_{Cc}$ copy, but not one with only the N-terminally FLAG-tagged $CdnL_{Cc}$ (FLAG-$CdnL_{Cc}$), suggesting that an N-terminal tag impairs $CdnL_{Cc}$ function. We therefore used strains expressing $cdnL_{Cc}$ from its native locus (to ensure normal growth) and the given FLAG-tagged $CdnL_{Cc}$ from a tightly controlled vanillate-inducible P_{van} promoter. To test if $CdnL_{Cc}$ is degraded in a ClpX-dependent manner *in vivo*, we introduced, as reported previously[35], a plasmid (pM088) allowing xylose-inducible expression of the dominant-negative ClpX* mutant chaperone (which is altered in its ATP-binding site and produces a catalytically dead ClpX form)[36]. Immunoblot analysis of FLAG-$CdnL_{Cc}$ degradation after turning off its expression (Fig. 2a) revealed that its stability was enhanced about two-fold when ClpX* expression was induced (estimated half-life of 45 ± 3 min, versus 18 ± 4 min when ClpX* was not induced). Moreover, $CdnL_{Cc}$-FLAG and FLAG-$CdnL_{Cc}$(DD), with the C-terminal AA motif masked or replaced by two aspartates, respectively, were considerably more stable whether or not ClpX* expression was induced (half-lives of ~300–580 min *in vivo*; Fig. 2a). Taken together, these results indicate that the AA motif at the C-terminus of $CdnL_{Cc}$ is an important determinant for its degradation *in vivo* and suggest that this might be dependent, at least in part, on ClpX.

C. crescentus undergoes asymmetric cell division to produce a non-replicative swarmer cell (SW) and a stalked cell (ST) that reinitiates the replicative cell cycle. Proper cell cycle progression depends on regulated proteolysis, often mediated by ClpXP[33,35]. The aberrant cell division phenotype caused by $CdnL_{Cc}$ depletion and the observation that it is subject to proteolysis prompted us to examine the levels of FLAG-$CdnL_{Cc}$ (expressed from P_{van}) along the cell cycle. As a control for synchronization and cell cycle progression, we also monitored the changes in the levels of CtrA, a master cell-cycle regulator and known ClpXP substrate, which is stable in SW cells, then gets degraded in ST cells and again reappears in predivisional (PD) cells[34,37,38]. FLAG-$CdnL_{Cc}$ increased from barely detectable levels in SW cells to peak at ~80 min (Fig. 2b). Interestingly, the clearance of FLAG-$CdnL_{Cc}$ from SW cells resembles that reported for the cell division protein FtsZ, a ClpXP and ClpAP substrate that, like $CdnL_{Cc}$, is stabilized by tagging its C-terminus or by mutating it to a DD motif[35].

The normal growth in the absence of vanillate of strain ME8, which expresses $CdnL_{Cc}$-FLAG from the native promoter and also bears a copy of $cdnL_{Cc}$ under P_{van} control, suggests that enhancing the stability of $CdnL_{Cc}$ and its resulting accumulation *in vivo* are not toxic to the cells (Fig. 2c). We confirmed this further with cells expressing only untagged $CdnL_{Cc}$(DD) that, like equivalent strains expressing only $CdnL_{Cc}$ or $CdnL_{Cc}$-FLAG, grew normally in the absence of vanillate on plates (Fig. 2c) or in liquid media (Fig. 2d). Thus, curiously, even though $CdnL_{Cc}$ is targeted for degradation *in vivo*, preventing this degradation by mutating the AA motif to DD or masking it with a C-terminal tag does not appear detrimental to *C. crescentus* growth or viability.

$CdnL_{Cc}$ interacts with itself and with RNAPβ. Full-length $CdnL_{Cc}$ is overall basic like $CdnL_{Tt}$, and not acidic like $CdnL_{Mx}$ or $CdnL_{Mt}$ (Supplementary Table S1). High-resolution tertiary structures determined for $CdnL_{Tt}$, $CdnL_{Mt}$ and $CdnL_{Mx}$ revealed a ~70-residue N-terminal β-sheet module and a C-terminal α-helical domain comprising the rest of the protein[16,18,19,22,39,40] that correspond well with sequence-based predictions of secondary structure (PSIPRED; http://bioinf.cs.ucl.ac.uk/psipred). Compared to its homologs, the putative $CdnL_{Cc}$ N-terminal domain is 32–39% identical and is also acidic (only in $CdnL_{Tt}$ it is basic), whereas its C-terminal domain, only 22–31% identical to the rest, is markedly basic, as in $CdnL_{Bs}$ (Supplementary Table S1). Despite the low sequence identity and the divergent overall domain charge distribution, the predicted $CdnL_{Cc}$ secondary structure (Supplementary Fig. S5) mirrors those in the high-resolution structures of $CdnL_{Tt}$, $CdnL_{Mt}$ and $CdnL_{Mx}$.

Interaction with cognate RNAPβ, a hallmark of most CdnL homologs studied thus far, was mapped to a solvent-exposed surface on the N-terminal β1 lobe of RNAPβ and to the ~70-residue N-terminal module in CdnL[9,16,21,39], which also mediates self-interactions[16,40]. Bacterial two-hybrid analysis (BACTH) confirmed that $CdnL_{Cc}$ conserves the ability to self-interact (Fig. 3a). A ~120 residue fragment of RNAPβ corresponding to the β1a subdomain (where residues critical for interaction with other CdnL homologs are located) was sufficient to detect interaction between $CdnL_{Mx}$ or $CdnL_{Tt}$ and their respective RNAPβ in BACTH[9,10]. However, in similar assays with other CdnL homologs, a longer ~500-residue fragment corresponding to the whole β1 domain

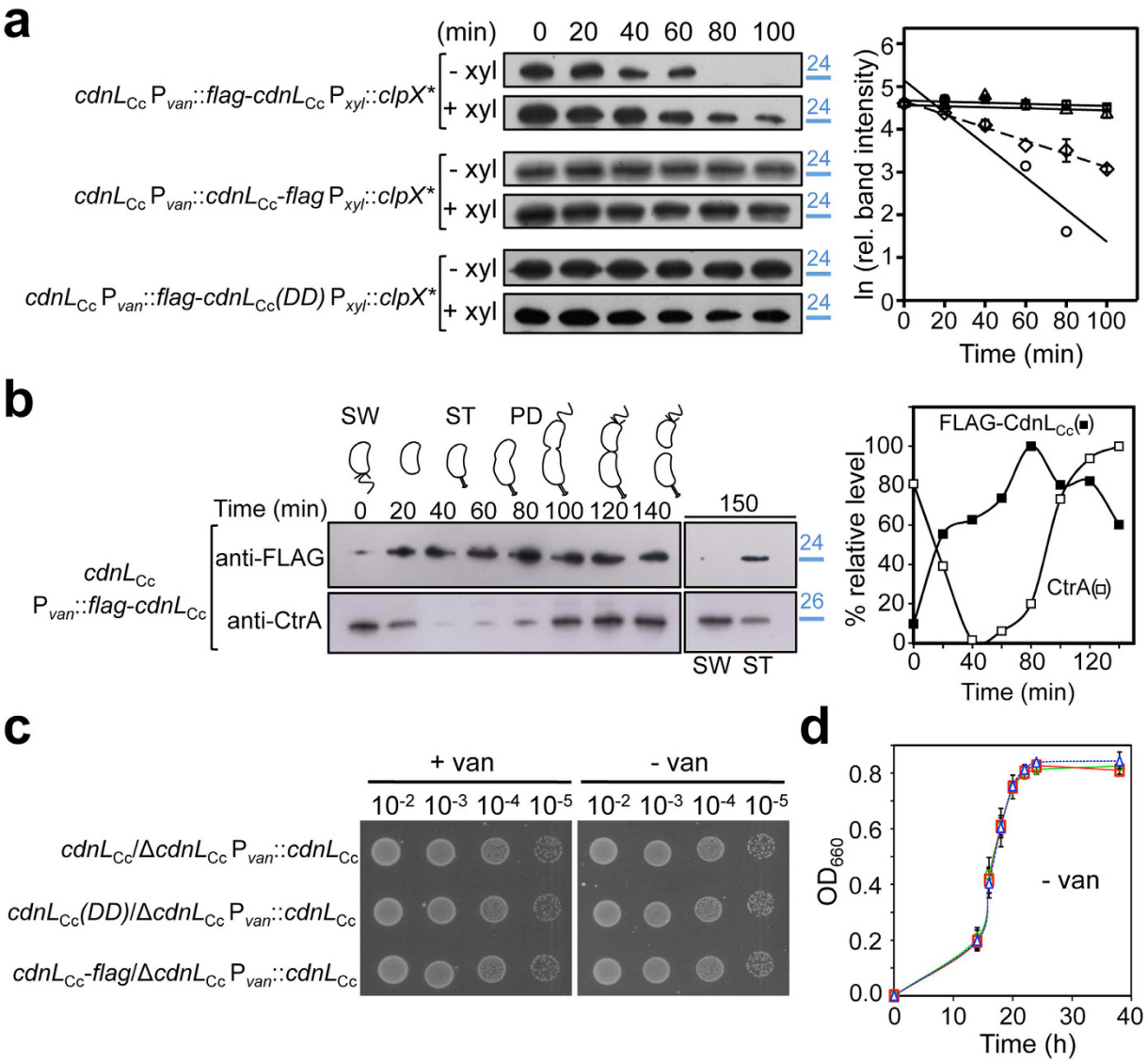

Figure 2. Analysis of $CdnL_{Cc}$ protein stability *in vivo*. (**a**) Stability of FLAG-$CdnL_{Cc}$, $CdnL_{Cc}$-FLAG and FLAG-$CdnL_{Cc}$(DD) *in vivo*. *C. crescentus* strains ME27, ME28 and ME29 were grown in PYE with vanillate, and subjected to a previously described protocol[35] (see Methods) prior to immunoblot analysis (−xyl: no xylose; +xyl: 0.3% xylose to induce *clpX** expression). Total protein from 1 ml aliquots withdrawn every 20 min was detected in immunoblots using anti-FLAG antibodies (left). On the right is a semi-log plot of the relative band intensities (mean of three independent experiments) versus time for FLAG-$CdnL_{Cc}$ (−xyl, circles; +xyl, diamonds), $CdnL_{Cc}$-FLAG (−xyl, triangles) and FLAG-$CdnL_{Cc}$(DD) (−xyl, squares). Slopes of the linear fits shown yield the decay rate constants used to estimate half-lives. (**b**) FLAG-$CdnL_{Cc}$ levels during the cell cycle. Swarmer cells (SW) from strain ME24 grown in M2G with vanillate were isolated and used for synchronized cell cycle progression (~150 min doubling time). Total protein from 1 ml aliquots taken every 20 min was subjected to immunoblot analysis using anti-FLAG antibodies. The control CtrA was probed on a separate blot (since its gel mobility is close to that of FLAG-$CdnL_{Cc}$) using anti-CtrA antibodies[38] and equivalent samples from the same experiment processed in parallel. Samples at 150 min correspond to SW and ST (with a small proportion of PD) cells isolated from the culture remaining at the end of this assay. A plot of band intensities (% of the maximum value) versus time is shown (right). In (**a**,**b**), positions of molecular size markers (kDa) are shown in blue to the right of cropped immunoblots. Note that FLAG-tagged $CdnL_{Cc}$ (~19.5 kDa calculated Mw) migrates slower than expected. (**c**) Growth of *C. crescentus* strains (ME41, ME39, ME8) expressing $CdnL_{Cc}$, $CdnL_{Cc}$(DD) or $CdnL_{Cc}$-FLAG, respectively, at the endogenous site. Liquid cultures (OD_{660} ~ 0.5) were serially diluted, spotted (8 μl) on PYE plates with or without vanillate, and incubated for 2 days at 30 °C. (**d**) Growth curves of strains in (**c**) expressing $CdnL_{Cc}$ (squares, red), $CdnL_{Cc}$-FLAG (triangles, blue) or $CdnL_{Cc}$(DD) (circles, green) in PYE without vanillate at 30 °C.

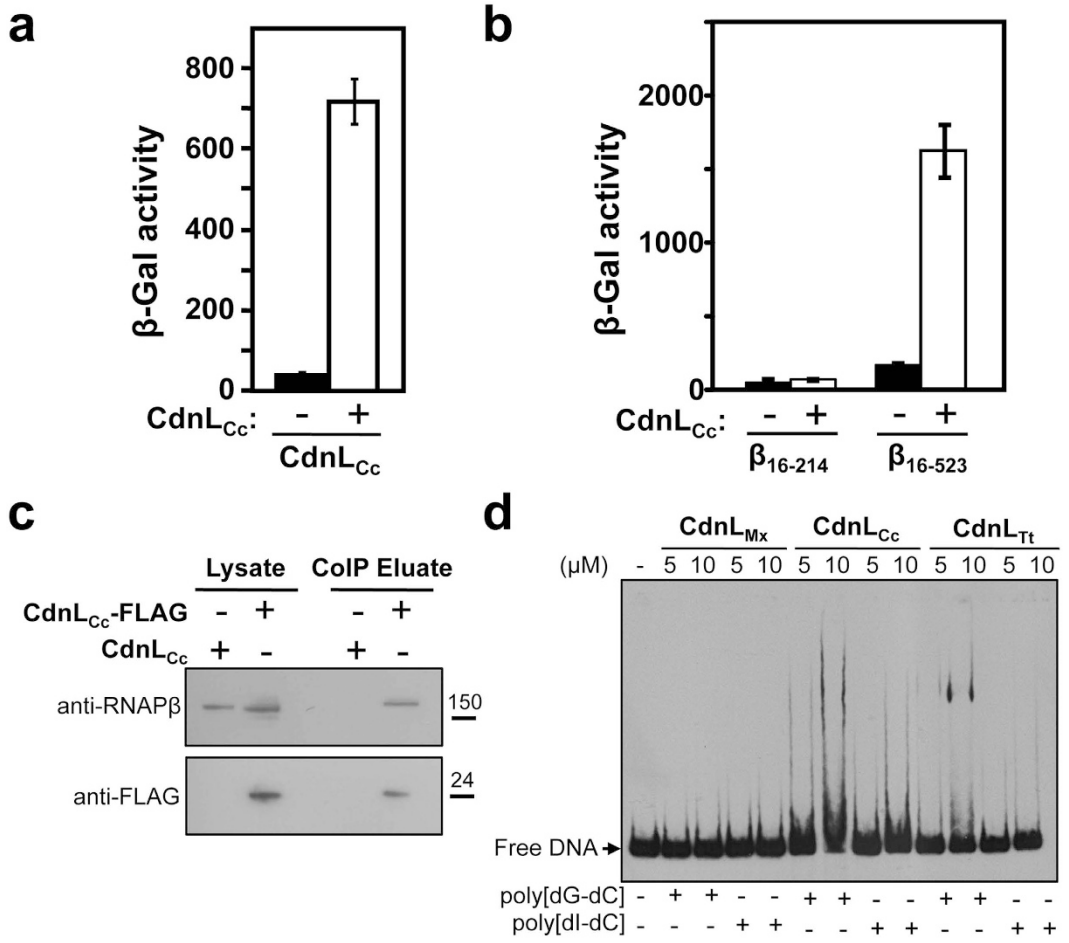

Figure 3. CdnL$_{Cc}$ interacts with itself, with RNAP, and with DNA. (**a**) BACTH analysis of CdnL$_{Cc}$ self-interaction in *E. coli* BTH101 transformed with plasmids pUT18-*cdnL*$_{Cc}$ and pKT25-*cdnL*$_{Cc}$. (**b**) BACTH analysis of the interaction between CdnL$_{Cc}$ (in pKT25) and *C. crescentus* RNAP β subunit fragments β$_{16-214}$ and β$_{16-523}$ (in pUT18C). In (**a**,**b**), the negative control (-) was pKT25 without insert. (**c**) Western blot of immunoprecipitated CdnL$_{Cc}$-FLAG probed for the presence of coprecipitating RNAPβ. Cells expressing CdnL$_{Cc}$-FLAG (strain ME17: Δ*cdnL*$_{Cc}$, P$_{van}$::*cdnL*$_{Cc}$-*flag*, *vanR*) or, as the negative control, untagged CdnL$_{Cc}$ (strain ME5: Δ*cdnL*$_{Cc}$, P$_{van}$::*cdnL*$_{Cc}$, *vanR*) were immunoprecipitated with anti-FLAG agarose and processed in parallel, as described in Methods. Equal amounts of sample were then resolved by SDS-PAGE for immunoblot analysis. Monoclonal anti-RNAP β antibodies were used to detect RNAPβ (top) that coimmunoprecipitated with CdnL$_{Cc}$-FLAG, which was detected using anti-FLAG antibodies (bottom). Molecular size markers are shown to the right of the cropped immunoblots by the lines and corresponding values in kDa. (**d**) EMSA for the DNA binding of CdnL$_{Cc}$, CdnL$_{Tt}$, and CdnL$_{Mx}$. Reactions were performed as described in Methods with a 350-bp P$_{rrnA}$ DNA probe, and with 1 μg of poly[dG-dC] or poly[dI-dC] added as nonspecific competitor.

(subdomains β1a and β1b) was required, likely because β1a alone does not always constitute a stable, well-folded domain[16,21]. Thus, to test the interaction between CdnL$_{Cc}$ and RNAPβ, a fragment encompassing only β1a (β$_{16-214}$) or the whole β1 domain (β$_{16-523}$) was used. Increased β-galactosidase activity with the β$_{16-523}$ fragment (Fig. 3b) suggests that CdnL$_{Cc}$ conserves the interaction with RNAPβ. To corroborate this interaction with RNAP in *C. crescentus*, we performed coimmunoprecipitation experiments with cells expressing CdnL$_{Cc}$-FLAG and, as a control, with equivalent cells expressing untagged CdnL$_{Cc}$ (see Methods). Detection of a band corresponding to RNAPβ by immunoblot analysis of cells expressing CdnL$_{Cc}$-FLAG confirmed the CdnL$_{Cc}$-RNAP interaction in *C. crescentus* (Fig. 3c).

CdnL$_{Cc}$ interacts nonspecifically with dsDNA. CdnL$_{Mt}$ has been reported to bind DNA nonspecifically *in vitro* through a positively charged patch at its C-terminal domain[39], although *in vivo* it was not found on the genome in the absence of RNAP[18]. However, direct DNA binding has never been observed for CdnL$_{Mx}$, which was proposed to associate with DNA exclusively via its interaction with RNAP[9,16]. CdnL$_{Mx}$ is overall acidic, as is CdnL$_{Mt}$ (Supplementary Table S1), whereas CdnL$_{Cc}$ is basic and could possibly bind to DNA and other polyanions. We therefore compared the DNA binding behaviour of CdnL$_{Cc}$, CdnL$_{Tt}$ (also basic) and CdnL$_{Mx}$ to a 350-bp double-stranded DNA probe that includes the promoter region of *rrnA* (P$_{rrnA}$), one of the two rRNA operons in *C. crescentus*. The probe incubated with CdnL$_{Cc}$ or CdnL$_{Tt}$ and without nonspecific competitor DNA present

precipitated in the loading well (not shown) suggesting nonspecific DNA binding. In the presence of nonspecific competitor DNA, a smeared retarded band could be discerned at high protein concentrations (5–10 μM) with $CdnL_{Cc}$ or $CdnL_{Tt}$, but not with $CdnL_{Mx}$, but most of the labeled DNA probe remained free (Fig. 3d). We mutated to Ala three basic residues in the C-terminal domain of $CdnL_{Cc}$ (Arg92, Arg93, Arg130) that align with those in the basic patch mentioned above (Supplementary Fig. S1). Binding to the DNA probe was weakened on mutating Arg130, and abolished on mutating both Arg92 and Arg93 (Supplementary Fig. S6a). Similar results were observed with a randomly chosen intragenic DNA probe *in vitro* (Supplementary Fig. S6b). Altogether, these data suggest that $CdnL_{Cc}$ can bind nonspecifically to DNA *in vitro*, largely via electrostatic interactions.

$CdnL_{Cc}$ depletion impairs rRNA transcription in *C. crescentus*. Our results thus far indicate that $CdnL_{Cc}$ is required for normal cell growth and that it interacts with RNAPβ, like most of its homologs that have been studied thus far. These have been shown to localize at promoters dependent on the primary σ factor, such as those for rRNA, and to activate them[15–19]. Hence, we used quantitative chromatin immunoprecipitation (ChIP) with anti-FLAG antibodies to probe if $CdnL_{Cc}$ localizes to P_{rrnA} (the *rrnA* operon promoter region) in *C. crescentus* by using cells expressing $CdnL_{Cc}$-FLAG (strain ME17) or $CdnL_{Cc}$ as negative control (strain ME5). This assay demonstrated that, relative to an intragenic region, $CdnL_{Cc}$ was indeed enriched at P_{rrnA}, as were the primary σ factor in *C. crescentus* (σ^{73}) or RNAPβ used as positive controls (Fig. 4a). We also found that $CdnL_{Cc}$ was enriched at two other σ^{73}-dependent promoters but not at one requiring σ^{F}, an alternative ECF σ factor in *C. crescentus*[25,41,42] (Supplementary Fig. S7). This suggests that $CdnL_{Cc}$, like the homologs studied, is associated with promoters that depend on the primary σ factor.

Next, we examined if $CdnL_{Cc}$ affects transcription *in vivo*, focusing on P_{rrnA}. We used a *C. crescentus* strain (ME42) that expresses $cdnL_{Cc}$ under P_{van} control and bears a transcription reporter plasmid with P_{rrnA} and the first 81 nucleotides of its leader fused to a *lacZ* gene fragment. This design is based on a previous study[43], which showed that transcription from this P_{rrnA} reporter was rapidly downregulated on glucose starvation, and proposed that this was mediated by an unknown factor. Such a factor could, in principle, be one that activates rRNA transcription but disappears rapidly on glucose starvation to swiftly lower rRNA transcription. $CdnL_{Cc}$ could potentially be this factor if it activates rRNA transcription, and if it becomes unavailable on glucose deprivation. Hence, we tested the effects of depleting $CdnL_{Cc}$ on P_{rrnA} transcription *in vivo* and whether this was affected on glucose deprivation.

Cells were grown to mid-log phase with vanillate, after which the inducer was eliminated to restrict $cdnL_{Cc}$ expression. This would result in a progressive drop in $CdnL_{Cc}$ levels over time due to intracellular degradation. Reporter P_{rrnA} transcription, estimated by qRT-PCR, decreased gradually after removal of vanillate, suggesting that $CdnL_{Cc}$ is directly or indirectly required for P_{rrnA} expression (Fig. 4b). Glucose deprivation caused a sharp drop in rRNA transcription, even right after removal of the inducer (Fig. 4b). To test if this is due to rapid degradation of $CdnL_{Cc}$, somehow triggered by glucose starvation, we repeated the above analysis in a strain (ME40) expressing the considerably more stable, yet functional, $CdnL_{Cc}$-FLAG. Rather than gradually decreasing over time, relative transcript levels observed in the presence of glucose now remained fairly steady over the 8 h period (Fig. 4c), consistent with $CdnL_{Cc}$-FLAG persisting even 8 h after removal of the inducer, albeit at lower levels (Fig. 4d). P_{rrnA} transcription again dropped dramatically on glucose starvation (Fig. 4c), even though $CdnL_{Cc}$-FLAG levels, at all time points, were comparable with or without glucose deprivation (Fig. 4d). Taken together these results indicate that depletion of $CdnL_{Cc}$ impairs rRNA expression, suggesting that $CdnL_{Cc}$ directly or indirectly promotes rRNA transcription *in vivo*, but that factors and mechanisms other than a rapid loss of $CdnL_{Cc}$ likely determine the sharp fall in rRNA expression occurring on glucose deprivation.

Missense mutations at conserved $CdnL_{Cc}$ residues cause cold sensitivity. The results thus far establish that $CdnL_{Cc}$ interacts with itself and with RNAPβ, localizes at P_{rrnA} and affects its activity. To test if the interaction with RNAPβ is required for $CdnL_{Cc}$ function in *C. crescentus*, two classes of mutations were generated, mimicking those reported previously in other CdnL homologs: mutations in the N-terminal module that disrupt the interaction with RNAP and those in the C-terminal domain that leave the interaction with RNAP intact[16,18,21,22].

$CdnL_{Cc}$ N-terminal residues Val39, Arg52, and Pro54 (Supplementary Fig. S1) were mutated to Ala, since equivalent mutations in $CdnL_{Mx}$, $CdnL_{Mt}$ or $CdnL_{Tt}$ caused loss of interaction with RNAPβ and, where tested, impaired cell growth[16,22,39]. BACTH indicated significantly reduced interaction of $\beta_{16\text{-}523}$ with mutants V39A and P54A, but not with R52A (Fig. 5a), indicating that $CdnL_{Cc}$ conserves at least two of the expected contacts with RNAPβ. To test the effect of the mutations in *C. crescentus*, plasmids bearing a given allele (expressing the protein with a C-terminal FLAG tag) flanked by ~500 bp genomic DNA upstream and downstream of $cdnL_{Cc}$ were introduced into strain ME5 (Fig. 5b). Transformants with plasmids integrated by homologous recombination at the endogenous $cdnL_{Cc}$ site were isolated in the presence of vanillate and then examined after removal of the inducer. On plates lacking vanillate, all three mutants grew normally at 30 °C (Fig. 5c). Notably, V39A and P54A functioned in *C. crescentus* despite their inability to interact with RNAPβ. By contrast, such mutations were lethal in *M. xanthus*[16] and in *M. tuberculosis*, but apparently not in *M. smegmatis*, closely related to *M. tuberculosis*[21]. Interestingly, we noticed that lowering the growth temperature from 30 °C to 25 °C under vanillate-free conditions caused significant growth arrest of V39A and P54A, while R52A, which continues to interact with RNAPβ, still grew normally (Fig. 5c). Consistent results were obtained for growth in liquid media without vanillate (Fig. 5d), with several cells of the poorly growing V39A and P54A mutants at 25 °C having the aberrant elongated cell morphology of a $\Delta cdnL_{Cc}$ strain (Fig. 5e). All of the mutant proteins were stable *in vivo* at both growth temperatures (Fig. 5f), implying that loss of function of V39A and P54A at the lower temperature does not stem from protein instability. This behavior does not appear to be caused by increased stability of $CdnL_{Cc}$ due to the C-terminal FLAG tag, since the cold sensitivity was also observed with the representative untagged P54A mutant

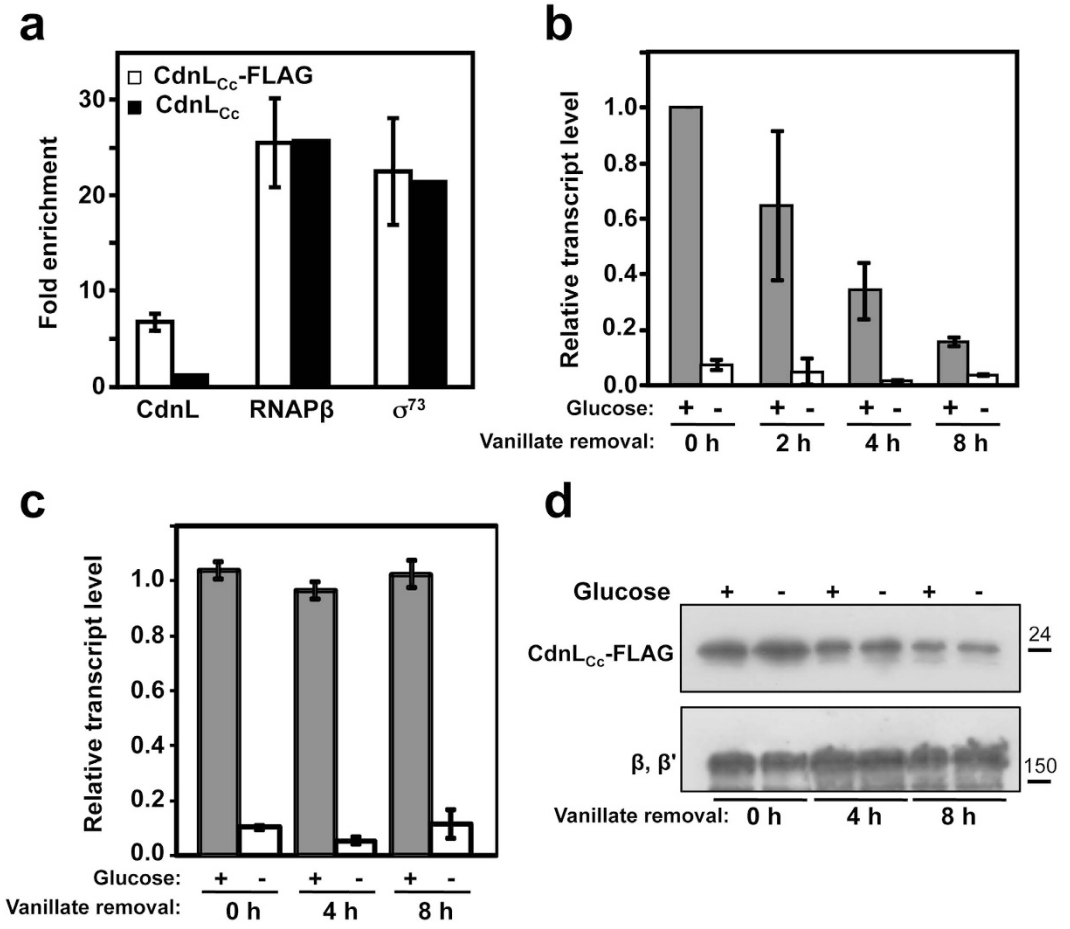

Figure 4. CdnL$_{Cc}$ localizes at an rRNA promoter and affects its transcription *in vivo*. (**a**) CdnL$_{Cc}$ binds to P$_{rrnA}$ *in vivo*. ChIP-qPCR analysis using an anti-FLAG antibody on cells expressing CdnL$_{Cc}$-FLAG (strain ME17: Δ*cdnL*$_{Cc}$, P$_{van}$::*cdnL*$_{Cc}$-*flag*, *vanR*; unfilled bars) or CdnL$_{Cc}$ as negative control (strain ME5: Δ*cdnL*$_{Cc}$, P$_{van}$::*cdnL*$_{Cc}$, *vanR*; black bars) showing CdnL$_{Cc}$-FLAG enrichment at P$_{rrnA}$ *in vivo*, relative to an intergenic region. As positive controls, ChIP-qPCR analysis was carried out using anti-RNAP β or anti-σ^{A} monoclonal antibodies for enrichment of RNAP or σ^{73}, respectively, at P$_{rrnA}$. (**b**) Effects of CdnL$_{Cc}$ depletion on P$_{rrnA}$ promoter activity *in vivo.* CdnL$_{Cc}$ was expressed from the P$_{van}$ promoter in strain ME42. Cells grown in M2G with vanillate to OD$_{660}$~0.4 were washed and then grown in vanillate-free medium to block *cdnL*$_{Cc}$ expression, and activity was measured by qRT-PCR at the times indicated. At each time point following vanillate withdrawal, one-half of the sample was washed and resuspended in medium without glucose and the other half remained untreated. Following 15 min incubation at 30 °C, the samples were collected for qRT-PCR analysis. (**c**) qRT-PCR analysis carried out with strain ME40, which expresses CdnL$_{Cc}$-FLAG from the P$_{van}$ promoter, using a procedure identical to that in (**b**). Data shown in (**a**–**c**) correspond to the mean and standard error from three biological replicates. (**d**) Immunoblot analysis of CdnL$_{Cc}$-FLAG corresponding to samples in (**c**) with and without glucose deprivation and at the times indicated following vanillate withdrawal (top). As loading control, the same blot was probed using polyclonal anti-RNAP antibodies; the band corresponding to the RNAP β, β′ subunits is shown (bottom). Molecular size markers are shown to the right of the cropped immunoblots by lines and corresponding values in kDa.

(Supplementary Fig. S8). Thus, interaction with RNAPβ does not appear to be critical for CdnL$_{Cc}$ function in *C. crescentus* except at lower than standard growth temperatures.

We next examined the effect of mutating Trp90, Arg92, Arg93, Tyr127 or Arg130 (Supplementary Fig. S1) in the CdnL$_{Cc}$ C-terminal domain, which is markedly basic and shares low sequence identity with its acidic counterparts in CdnL$_{Mx}$, CdnL$_{Mt}$ and/or CdnL$_{Tt}$ (Supplementary Table S1). Nonetheless, CdnL$_{Cc}$ residues Trp90, Arg93, and Arg130 are conserved in all four homologs, Arg92 is conserved in CdnL$_{Mx}$ and CdnL$_{Mt}$, and Tyr127 is a Phe in CdnL$_{Mx}$. With CdnL$_{Mx}$, CdnL$_{Mt}$ or CdnL$_{Tt}$, mutational data had shown these residues to be functionally important in at least one of the homologs; and high-resolution structures revealed the residues to be part of a solvent-exposed basic-hydrophobic patch[16,18,39,40]. Moreover, in the crystal structure of the RP$_o$-CdnL$_{Tt}$ complex, Trp86 was in a position to interact with a highly conserved thymine (T$_{12}$) at the upstream edge of the DNA bubble, and act as a wedge to prevent bubble collapse; and CdnL$_{Tt}$ activity *in vitro* was shown to require Trp86 and T$_{12}$[19]. Interestingly, mutating this highly conserved tryptophan impaired growth in *M. tuberculosis* but not in *M. smegmatis*[44] or in *M. xanthus*[16].

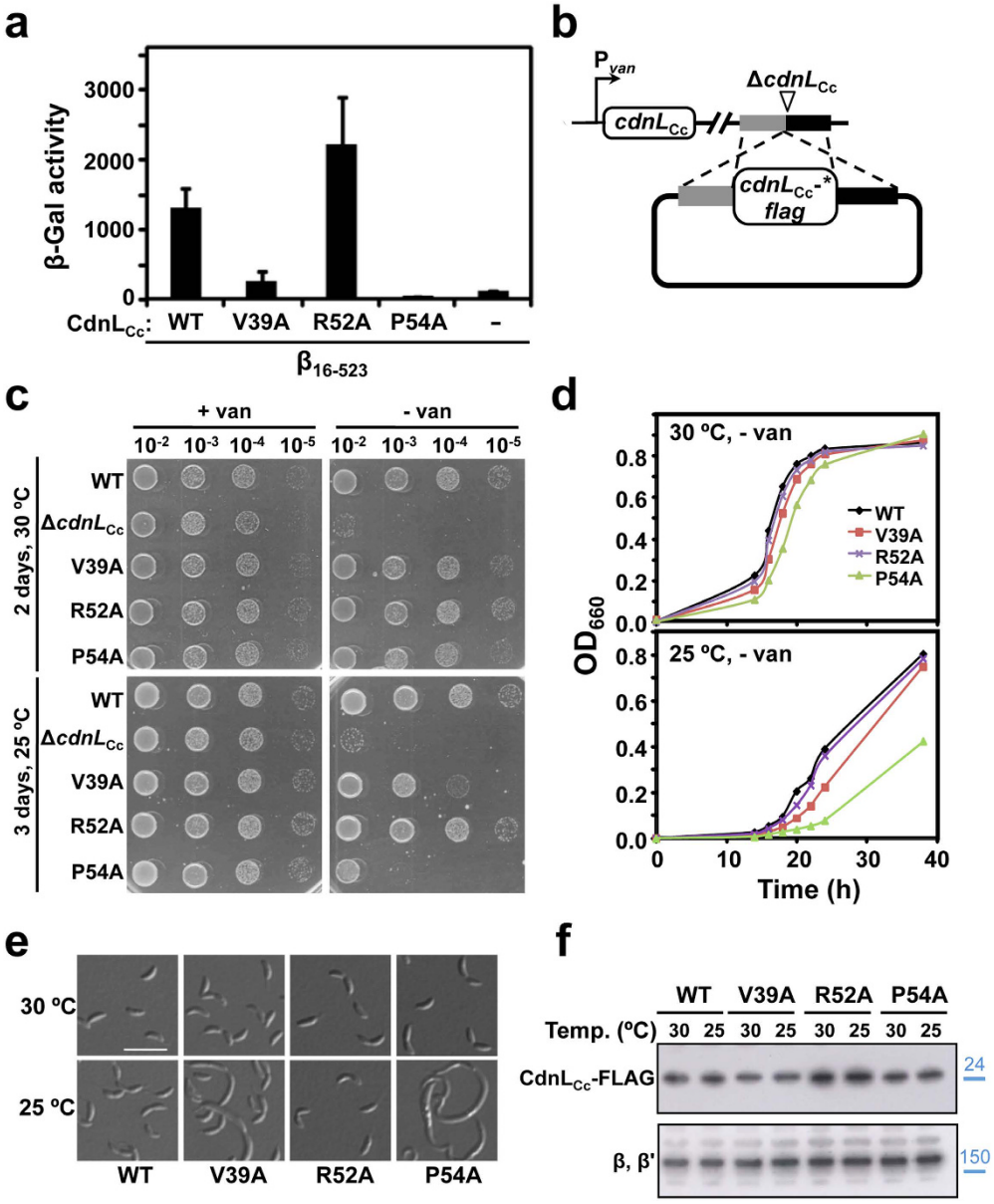

Figure 5. Mutational analysis of CdnL$_{Cc}$-RNAP interaction *in vivo*. (**a**) BACTH analysis of the interaction of CdnL$_{Cc}$ mutants V39A, R52A and P54A (in pKT25) with *C. crescentus* RNAPβ fragment β$_{16-523}$ (in pUT18C). The negative control (–) bears empty pKT25 and pUT18C-β$_{16-523}$. (**b**) Schematic for the strategy employed to check for *cdnL$_{Cc}$* complementation in *C. crescentus*. A pMR3552 derivative with the required *cdnL$_{Cc}$-flag* allele (* indicates mutant) flanked by DNA segments upstream (grey) and downstream (black) of *cdnL$_{Cc}$* in the genome was introduced into strain ME5, which bears the Δ*cdnL$_{Cc}$* allele at the endogenous site and P$_{van}$-*cdnL$_{Cc}$* at a heterologous site. Merodiploids resulting from plasmid integration by recombination express both CdnL$_{Cc}$*-FLAG and CdnL$_{Cc}$ in the presence of vanillate (+van) and only the former in the absence of vanillate (−van). (**c**) Complementation analysis in *C. crescentus* of cells bearing the Δ*cdnL$_{Cc}$* allele or ones expressing at the endogenous site C-terminal FLAG-tagged wild-type CdnL$_{Cc}$ (WT) or the indicated N-terminal CdnL$_{Cc}$ variants. PYE plates with (+van) or without (−van) vanillate were spotted with 8 μl of liquid cultures (OD$_{660}$ ~ 0.5) at the dilutions indicated and incubated at 30 °C for two days or at 25 °C for three days. (**d**) Growth curves at 30 °C or 25 °C of *C. crescentus* expressing C-terminal FLAG-tagged CdnL$_{Cc}$ (WT) or its indicated variants cultivated in liquid PYE without vanillate using the procedures described in Fig. 1b. (**e**) Cellular morphology examined by DIC microscopy of the wild-type (WT; scale bar: 5 μm) and the indicated mutant cells from (**d**) grown at 30 °C or 25 °C. (**f**) Immunoblot analysis to probe the stability of N-terminal CdnL$_{Cc}$ variants. Cell extracts of strains expressing C-terminal FLAG-tagged CdnL$_{Cc}$ (WT) or its indicated variants grown at 30 °C or 25 °C in PYE with vanillate were probed using anti-FLAG antibodies (top). As loading control, the same blot was probed using polyclonal anti-RNAP antibodies; the band corresponding to the RNAP β, β′ subunits is shown (bottom). Molecular size markers are shown to the right of the cropped immunoblots by lines and corresponding values in kDa (in blue).

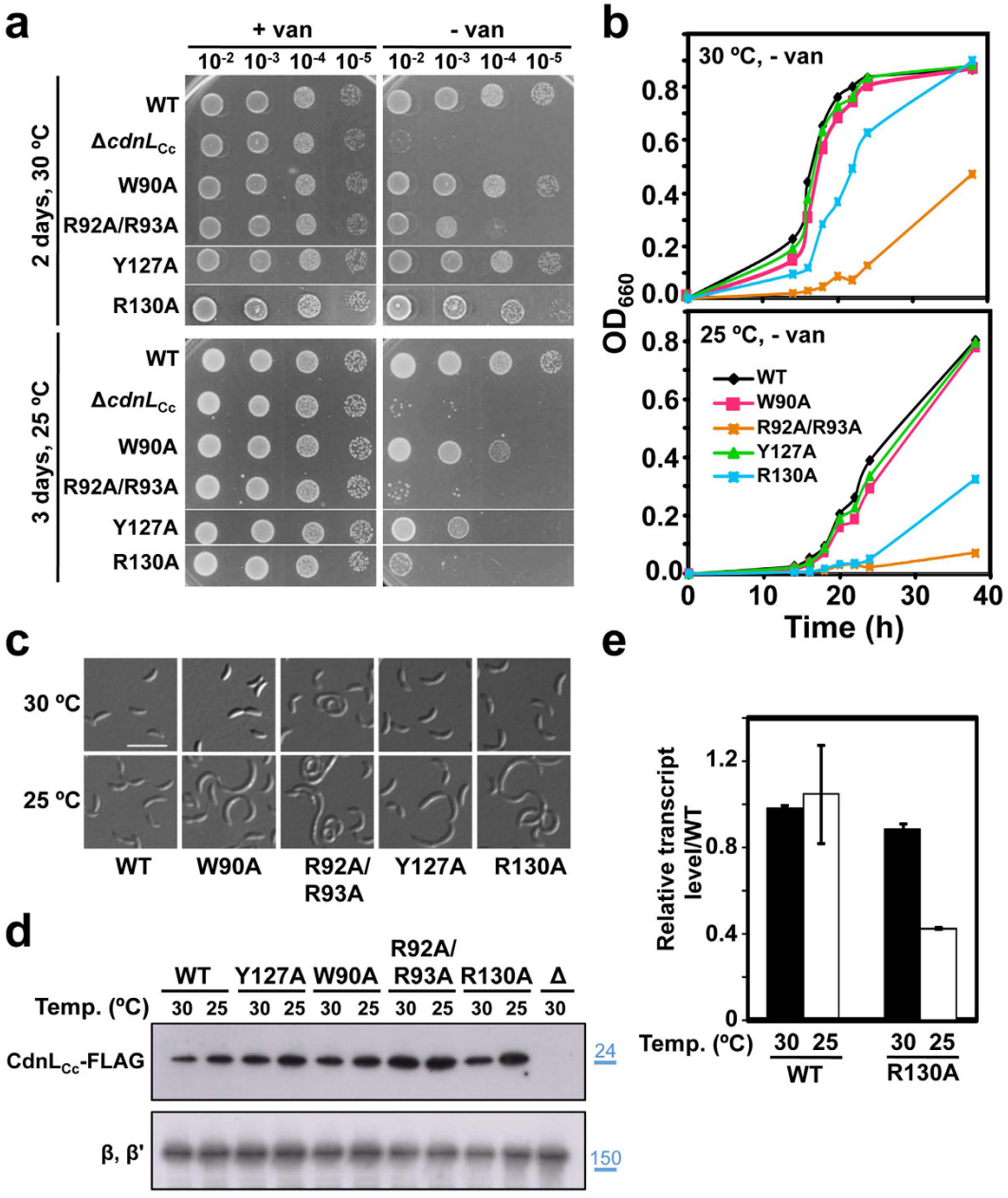

Figure 6. Analysis of C-terminal $CdnL_{Cc}$ mutations *in vivo*. (**a**) Complementation analysis in *C. crescentus* of cells bearing the Δ*cdnL*$_{Cc}$ allele or ones expressing at the endogenous site C-terminal FLAG-tagged wild-type $CdnL_{Cc}$ (WT) or the indicated C-terminal $CdnL_{Cc}$ variants. The analysis was carried out using the same procedures and conditions described in Fig. 5c. (**b**) Growth curves at 30 °C or 25 °C of *C. crescentus* strains expressing the C-terminal FLAG-tagged $CdnL_{Cc}$ (WT) or its indicated variants cultivated in liquid PYE without vanillate using the procedures described in Fig. 1b. (**c**) Cellular morphology examined by DIC microscopy of the wild-type (WT; scale bar: 5 μm) and the indicated mutant cells from (**b**) grown at 30 °C or 25 °C. (**d**) Immunoblot analysis to probe the stability of C-terminal $CdnL_{Cc}$ variants. Cell extracts of strains expressing C-terminal FLAG-tagged wild-type $CdnL_{Cc}$ (WT) or the indicated $CdnL_{Cc}$ mutants grown at 30 °C or 25 °C in PYE with vanillate were probed using anti-FLAG M2 antibodies (top). The negative control "Δ" corresponds to the strain (ME5) with the Δ*cdnL*$_{Cc}$ allele at the endogenous site and expressing untagged $CdnL_{Cc}$ under P_{van}. As loading control, the same blot was probed using polyclonal anti-RNAP antibodies; the band corresponding to the RNAP β, β′ subunits is shown (bottom). Molecular size markers are shown to the right of the cropped immunoblots by lines and corresponding values in kDa (in blue). (**e**) P_{rrnA} promoter activity *in vivo* at 30 °C or at 25 °C in cells expressing $CdnL_{Cc}$-FLAG (WT) or its variant with the R130A mutation under P_{van} control (strains ME40 and ME38, respectively). Cells grown overnight at 30 °C in M2G with vanillate were diluted into the same medium to $OD_{660} \sim 0.1$. One-half was grown at 30 °C and the other at 25 °C to OD_{660} of 0.3–0.4, and RNA was quantitated using qRT-PCR. Data shown correspond to the mean and standard error from three biological replicates.

The $CdnL_{Cc}$ C-terminal mutants tested grew normally at 30 °C in the absence of vanillate, except for the double R92A/R93A mutant, which did show a growth defect (Fig. 6a). In comparison, the *M. xanthus* mutant corresponding to $CdnL_{Cc}$ R92A/R93A also grew very poorly while that equivalent to Y127A showed somewhat impaired growth[16], and single mutations of a number of these residues caused lethality in *M. tuberculosis* but not in the closely related *M. smegmatis*[44]. Lowering the *C. crescentus* incubation temperature to 25 °C exacerbated the phenotype of the R92A/R93A mutant, caused somewhat deficient growth of W90A and Y127A, and a marked decrease in growth for R130A (Fig. 6a). Consistent results were obtained in liquid cultures lacking vanillate (Fig. 6b), and several cells of the mutants growing poorly at 25 °C had the abnormal elongated morphology (Fig. 6c). Again, the cold sensitivity does not appear to be due to protein instability (Fig. 6d), or entirely to protein stabilization resulting from the presence of the C-terminal tag, since the R130A mutant without the tag remained cold sensitive, albeit to a lower extent (Supplementary Fig. S8). Relative levels of reporter rRNA estimated by qRT-PCR were comparable for R130A and wild type at 30 °C but dropped significantly for the mutant at 25 °C (Fig. 6f), suggesting that impaired growth correlates with diminished rRNA transcription.

In sum, our data suggest that both classes of functionally important mutations are conserved in $CdnL_{Cc}$ but they cause cold-sensitive phenotypes in *C. crescentus*.

Discussion

Experimental validation of function for different proteins of the same family is required not only to gain insights into structure-function relationships but also because of several examples of apparently sequence-related proteins shown to be functionally distinct. Thus, CarD and CdnL have different functions, despite various shared structural features and interactions. $CdnL_{Mx}$ and $CdnL_{Mt}$ are similar in their essentiality, structure, and function in stabilizing RP_o formation and activating rRNA transcription, whereas $CdnL_{Bs}$ lacks these properties. The fact that nearly all alphaproteobacteria have a CdnL homolog, with those of *C. crescentus* and a few other alphaproteobacteria being listed as essential based on genome-wide Tn-Seq studies[29–31], prompted us to study $CdnL_{Cc}$. We have shown here that $CdnL_{Cc}$ is not essential, unlike $CdnL_{Mt}$ and $CdnL_{Mx}$, but that its depletion leads to slow growth and cell filamentation in *C. crescentus*. The slow growth probably explains why $CdnL_{Cc}$ was listed among the essential *C. crescentus* proteins[29], just as in the case of SsrA, GcrA and CcrM, which were initially deemed to be essential in *C. crescentus* but subsequently shown to be dispensable[45–47]. Despite this key difference from its myco/myxobacterial homologs, $CdnL_{Cc}$ nevertheless conserves the interaction with RNAP and other functional determinants, and directly or indirectly affects rRNA transcription, reinforcing the evidence for an important, broadly conserved regulatory role of CdnL in bacteria.

Both $cdnL_{Mx}$ and $cdnL_{Mt}$ are expressed from a primary σ-dependent promoter with a short 5′-UTR. While $cdnL_{Mt}$ is sharply and quickly upregulated upon starvation or exposure to some other stresses[10], this has not been observed for $cdnL_{Mx}$[9]. On the other hand, $cdnL_{Bs}$ and *B. burgdorferi cdnL* expression was reportedly induced at lower temperatures from promoters that remain uncharacterized[11,48]. We found that expression of $cdnL_{Cc}$ increases during exponential growth and appears to be maintained in stationary phase. Global 5′-RACE data for *C. crescentus*[25] and *S. meliloti*[28] list their *cdnL* homologs among those genes dependent on the primary σ factor, but unlike $cdnL_{Mx}$ or $cdnL_{Mt}$, both alphaproteobacterial *cdnL* have 5′-UTRs >200-bp long. The *S. meliloti cdnL* 5′-UTR was reported to contain also a heat-shock σ^H promoter[28,49], but we did not find any appreciable change in $cdnL_{Cc}$ expression upon heat shock (Supplementary Fig. S9), suggesting absence of a σ^H promoter in the $cdnL_{Cc}$ 5′-UTR. We found that the intergenic region at the 5′ end of *cdnL* tends to be unusually long in alphaproteobacteria: >200 bp for >60% of the homologs with an overall median of 312 bp. Short 5′ intergenic sequences are only found in the Rickettsiales, which are well known for reductive evolution[50]. A long 5′-UTR may therefore be a common feature for *cdnL* in alphaproteobacteria. Future studies could shed light on the exact role of the long 5′-UTR, if any, on $cdnL_{Cc}$ expression.

Our data indicate that $CdnL_{Cc}$ is targeted for proteolysis *in vivo* in a manner dependent on its C-terminal AA motif, and is stabilized against intracellular degradation if this motif is masked by a C-terminal tag or is mutated to DD. This is a characteristic of many ClpXP-dependent substrates, and $CdnL_{Cc}$ degradation was reduced about two-fold upon expressing a dominant-negative ClpX variant that is known to inhibit ClpXP activity[35,36]. While this suggests that $CdnL_{Cc}$ may be degraded in a ClpXP-dependent manner in *C. crescentus*, we cannot rule out other mechanisms also operating, such as through the ClpAP protease, as has been observed for other proteins[35]. $CdnL_{Cc}$ levels (in cells expressing FLAG-$CdnL_{Cc}$ under P_{van} control) were barely detectable in non-replicative SW cells but easily detectable in ST and PD cells, suggesting that $CdnL_{Cc}$ may be subject to cell cycle-dependent proteolytic control, with a possible role in actively dividing cells. Interestingly, changes in $CdnL_{Cc}$ levels during the cell cycle are akin to those reported for the cell division protein FtsZ, a ClpXP and ClpAP substrate that also becomes stabilized if its C-terminus is tagged or mutated to DD[35]. We found that >80% of the alphaproteobacterial CdnL homologs have a C-terminal AA or VA, including those found in early diverging groups like the Rickettsiales. Hence, proteolysis of CdnL might be a common and conserved ancestral mechanism in alphaproteobacteria. $CdnL_{Mt}$, with a C-terminal AAAS has been shown to be a target of the essential Clp protease in *M. tuberculosis*, a phylum distinct from alphaproteobacteria[51], suggesting that Clp-mediated CdnL turnover might be a general feature. If so, this would hint at a crucial role for degradation of CdnL for post-translational control of its intracellular levels. However, it appears that degradation of $CdnL_{Cc}$ is not required for normal growth under standard conditions, but might instead be more important under some other untested conditions. Increased intracellular levels of CdnL in *M. tuberculosis*[51] or *M. xanthus*[9] are not harmful either. Cells thus appear to cope well with high CdnL concentrations under standard growth conditions.

Depleting $CdnL_{Cc}$ correlates with decreasing rRNA transcription and hence rapid degradation of $CdnL_{Cc}$ could, in principle, be a mechanism for the sharp drop in rRNA transcription that occurs *in vivo* upon glucose starvation in *C. crescentus*[43]. Our finding that this decrease occurs even when $CdnL_{Cc}$ is present at significant levels (due to dysregulation of its proteolysis) points to other mechanisms, as yet unidentified, for downregulating

rRNA expression upon glucose limitation. An interesting parallel to this has been reported for *E. coli* DksA, which is a ClpXP substrate[52] that inhibits rRNA transcription. Here, stabilization and a rapid accumulation of DksA on starvation could in theory swiftly reduce rRNA expression, but this is actually achieved by modulating the amounts of small cofactors like (p)ppGpp and NTPs[53].

An interesting finding of our study is the cold-sensitive phenotype associated with missense mutations in $CdnL_{Cc}$. Cold sensitivity was observed with N-terminal $CdnL_{Cc}$ mutations that disrupt interaction with RNAPβ, as well as with C-terminal ones that retain this interaction. By contrast, equivalent mutations in $CdnL_{Mx}$ or $CdnL_{Mt}$ impaired the essential function of CdnL even under standard growth conditions[16,21,44]. *In vitro* and structural studies have linked CdnL function to RP_o stabilization by preventing collapse of the transcriptional bubble[15–19]. Defective RP_o stabilization by CdnL mutants with the N-terminal mutations could be attributed to their lack of RNAP-binding and hence poor recruitment to RP_o (or RP_c), and by CdnL mutants with C-terminal mutations to their inability to accelerate DNA opening and inhibit bubble collapse (they interact with RNAP and are recruited to RP_o and RP_c like wild-type CdnL)[17]. Since $CdnL_{Cc}$, like $CdnL_{Mt}$ or $CdnL_{Mx}$, binds to an rRNA promoter and affects its expression *in vivo*, it may also function in stabilizing RP_o formation. If so, temperature-dependent effects on RP_o formation and intrinsic differences between CdnL homologs and/or RNAP could possibly underlie the cold sensitivity displayed by $CdnL_{Cc}$ point mutants. Lower temperatures are known to disfavor RP_o, which forms *via* a series of conformational changes, starting from RP_c assembly to melting of the promoter region between positions −11 and +2 relative to the TSS[2,3]. Also, the stabilizing effect *in vitro* of $CdnL_{Mt}$ on RP_o is more noticeable at 25 °C than at lower (10 °C) or higher (37 °C) temperatures, presumably because at 25 °C the energy landscape between RP_c and RP_o is more balanced and the additional binding energy provided by $CdnL_{Mt}$ significantly drives the equilibrium towards RP_o formation[15,17].

Our analysis highlights differences between $CdnL_{Cc}$ and its homologs, consistent with CdnL-RNAP interactions being species-specific[16], but how these translate into the observed cold-sensitive phenotype remains elusive. Significant differences in the stability of the complexes formed by different RNAP on the same promoters reveal mechanistic differences across bacterial species. Thus, the occurrence of CdnL has been correlated to the cognate RNAP forming an unstable RP_o and, tellingly, CdnL is absent in *E. coli* whose RNAP appears to form more stable RP_o than mycobacterial RNAP[15]. Relative to *M. xanthus* and mycobacteria, *C. crescentus* RNAP could form intrinsically more stable RP_o, such that lower temperature, on its own unfavorable for RP_o formation, is necessary to detect the debilitating effects of $CdnL_{Cc}$ mutations on RP_o stabilization. *In vitro* analyses using purified *C. crescentus* RNAP and $CdnL_{Cc}$, an aim for future work, should elucidate this further. Species-specific variations will necessarily have to be invoked to rationalize why *B. subtilis*, with an RNAP that forms unstable RP_o[54], has a CdnL that is not essential and that does not bind to RNAP or regulate rRNA transcription[12,13].

In conclusion, our study indicates that *C. crescentus* CdnL is not essential but is nonetheless required for normal growth and morphology, and is likely to be involved in rRNA transcription. The functional role of CdnL therefore appears to be fairly conserved in bacteria. It also highlights species-specific mechanistic differences for this factor relative to some of its homologs, within an otherwise preserved mode of action, that will be useful in understanding the structure-function relationships governing this class of important, RNAP-binding transcriptional regulators.

Methods

Strains, plasmids, and growth conditions. Strains and plasmids used in this study are listed in Supplementary Tables S2 and S3, respectively. Growth conditions, and strain and plasmid construction are detailed in Supplementary Methods in the Supplementary information file.

Bacterial two-hybrid (BACTH) analysis. The *E. coli* BACTH system used is based on functional complementation of the T25 and T18 fragments of the *Bordetella pertussis* adenylate cyclase catalytic domain when two test proteins interact[55]. Coding regions selected were PCR-amplified and cloned into the XbaI and BamHI sites of pKT25, pUT18 or pUT18C (Supplementary Table S3). Given pairs of pKT25 and pUT18/pUT18C constructs were electroporated into *E. coli* strain BTH101 (*cya*$^-$), a pair with a vector lacking an insert was the negative control. Interaction was assessed from measurements (mean and standard error of at least three experiments) of β-galactosidase specific activity (β-gal activity, in nmol of *o*-nitrophenyl β-D-galactoside hydrolysed/min/mg protein) from liquid cultures, as described[56].

Protein purification. His_6-tagged $CdnL_{Cc}$ and its variants were overexpressed from pET15b (Novagen) constructs as soluble, native proteins using procedures described for $CdnL_{Mx}$ and $CdnL_{Tt}$[16]. After thrombin digestion to remove the His_6-tag, the sample was passed through a phosphocellulose column equilibrated with 100 mM NaCl, 50 mM phosphate pH 7.5, 2 mM β-mercaptoethanol, eluted at 0.4 M NaCl, purified by size-exclusion (Superdex200, GE Health Sciences), and concentrated with Amicon Ultra (10000 MWCO from Millipore). Protein concentrations were estimated from absorbance at 280 nm using $\varepsilon_{280}(M^{-1}cm^{-1})$ determined from the sequence (http://web.expasy.org/protparam/).

Microscopy. At different times during growth, samples were withdrawn and the fluorescent dye 4′-6-diamino-2-phenylindole (DAPI; 350 nm excitation maximum, 461 nm emission maximum) was added to a final concentration of 1 ng/μl. A 1 μl drop applied on 1% agarose pads of M2 salts was examined under a Nikon Eclipse 80i microscope equipped with a Plan Apo VC 100×/1.40 oil immersion objective, and a Hamamatsu ORCA-AG CCD camera. A Nikon UV-2E/C filter set was used for DAPI fluorescence. Images were processed with Metamorph 4.5 (Universal Imaging Group) and Photoshop 6.0 (Adobe Systems).

Western blot and *in vivo* degradation analysis. Immunoblot analysis in whole cell extracts of $CdnL_{Cc}$ tagged with the FLAG epitope was carried out using standard procedures[9]. Total protein was estimated prior

to the analysis and aliquots with equal amounts of protein were resolved in 10% SDS-PAGE gels, transferred to Hybond-ECL membranes, and probed using the ECL system and anti-FLAG M2 monoclonal antibodies (F3165, Sigma-Aldrich). As loading control, the same blot was probed for RNAP (subunits β/β′) using polyclonal *B. subtilis* RNAP holoenzyme antibodies[57]. To test the possibility that $CdnL_{Cc}$ is degraded in a ClpX-dependent manner *in vivo*, we employed a previously established protocol[35]. Basically, the *C. crescentus* strain was grown in PYE with appropriate antibiotics and 0.5 mM vanillate overnight at 30 °C, diluted to an $OD_{660} = 0.1$ into 20 ml of the same medium, grown to an OD_{660} of 0.4 and divided into two 10 ml cultures. To one, glucose was added to 0.2% final concentration and, to the other, 0.3% xylose to induce *clpX**. After 2 h, cells were harvested by centrifugation, washed with 10 ml inducer-free PYE, and suspended in 10 ml fresh inducer-free media. Aliquots (1 ml) withdrawn at 20-min intervals were subjected to immunoblot analysis using anti-FLAG M2 antibodies. Relative band intensities were quantified by densitometry using the ImageJ software program and recommended protocols (NIH). Briefly, bands plus background were selected and a profile plot was obtained for each band (peaks). The straight-line tool was used to minimize background noise by closing off each peak above the baseline of the corresponding profile plot and to adjust the closing at the base of the peak in the case of spill-over signals, and the wand tool was used to quantify the closed peaks. The average and standard error of three independent experiments were used in further analysis. The slope of a linear fit to a plot of the natural logarithm of the relative band intensity (in % normalized to the zero time point) versus time using Sigmaplot (Systat Software Inc) yielded the decay rate and error, and the half-life was determined as ln(2)/-rate. To examine changes during the cell cycle (see Supplementary Methods), aliquots were withdrawn from synchronized cell cultures expressing FLAG-$CdnL_{Cc}$ (strain ME24 grown in the presence of 0.5 mM vanillate) every 20 min, inspected by microscopy for progression of the cell cycle, and analyzed in Western blots using anti-FLAG M2 or anti-CtrA antibodies[38], as a control for the synchronization protocol.

Electrophoretic mobility shift assays (EMSA). EMSA was carried out as described previously[16]. EMSA samples (20 μl) contained 1 nM ^{32}P-5′-end radiolabeled, double-stranded DNA probe (13,000 cpm) obtained by PCR and 5 or 10 μM protein in EMSA buffer (80 mM KCl, 25 mM Tris pH 8.0, 5 mM $MgCl_2$, 1 mM dithiothreitol, 10% glycerol, 200 ng/ml bovine serum albumin) with 1 μg of poly[dG-dC] or poly[dI-dC] as nonspecific competitor, as indicated. Samples were incubated for 30 min at 37 °C and electrophoresed at 200 V for 1.5 h in 4% nondenaturing PAGE gels in TBE buffer (45 mM Tris-boric acid, 1 mM EDTA) at 10 °C, after which the gel was vacuum dried and analyzed by autoradiography.

RNA isolation and qRT-PCR analysis. Cells expressing P_{van}-$cdnL_{Cc}$ or P_{van}-$cdnL_{Cc}$-*flag* were grown in 10 ml M2G medium with appropriate antibiotics and 0.5 mM vanillate (M2G-vanillate) overnight at 30 °C. 1 ml of this was innoculated into fresh 50 ml M2G-vanillate and grown to an $OD_{660} = 0.3–0.4$. Two 4 ml aliquots were withdrawn (time "0") and pelleted. One was stored at −80 °C until further processing. The other was washed twice with M2-vanillate (lacking glucose) to eliminate the glucose, resuspended in 4 ml M2-vanillate and grown at 30 °C for 15 min, then pelleted and stored at −80 °C until use (time "0", no glucose). The rest of the 50 ml culture was washed twice with M2G to eliminate vanillate, resuspended in 42 ml of fresh M2G with appropriate antibiotics and incubated at 30 °C. 4 ml aliquots were withdrawn at specific times (2, 4, 8 hours) and treated as with time "0" samples with and without glucose starvation. RNA was extracted from each sample using PureLink RNA Mini Kit (Thermo Fisher Scientific), treated with Turbo DNase (Ambion) for 4 h at 37 °C, and purified using the PureLink RNA Mini Kit. RNA levels were assessed by gel electrophoresis and with NanoDrop ND-1000 (Thermo Fisher Scientific) using a 260 nm extinction coefficient of 40 ng-cm/μl. 2 μg of total RNA was reverse transcribed into cDNA using random hexamer primers (Promega) and Transcriptor Reverse Transcriptase (Roche) in 20 μl of reaction mix as per manufacturer's instructions. 1 μl of cDNA was added to 10 μl SYBR Green PCR Master Mix (Applied Biosystems or BioRad), with the required primers (100 nM). Each reaction was performed in triplicate, with a control reaction using equivalent starting volume of RNA to verify absence of contaminating DNA. Primers to amplify an ~50–150 bp region within each transcript were designed using Primer Express 3.0 software, and qRT-PCR was carried out in a StepOne instrument and software using the 1-Step RT-PCR program cycle without reverse transcription (Applied Biosystems). Melting and dissociation curves were determined from 60–95 °C, 30s and 95 °C, 15s. Primers to quantify 16S rRNA transcription from the P_{rrnA}::*lacZ* reporter plasmid pMR3769 and of *ruvA* (as endogenous control) are those described previously[43], and their ratio yields the 'Relative transcript level' for each sample. For each primer pair a standard RT-PCR curve was generated for five serial ten-fold dilutions of cDNA, and ones with near 100% efficiency were used.

Coimmunoprecipitation (CoIP). Strains ME5 (Δ$cdnL_{Cc}$, P_{van}::$cdnL_{Cc}$, *vanR*) and ME17 (Δ$cdnL_{Cc}$, P_{van}::$cdnL_{Cc}$-*flag*, *vanR*) were grown in 500 ml PYE with appropriate antibiotics and 0.5 mM vanillate to OD_{660} of ~0.3, harvested by centrifugation, washed thrice with CoIP buffer (20 mM HEPES pH 7.5, 50 mM NaCl, 20% glycerol), and the pellets frozen at −80 °C until further use. Frozen pellets were resuspended in 5 ml CoIP buffer, incubated with 10 mM $MgCl_2$, 50 mg lysozyme and 50 units DNase I (Promega) at 4 °C with shaking for 30 min, lysed with a French press at 16,000 psi, and clarified by centrifugation (18,000 *g*, 4 °C, 5 min). Cleared lysates were incubated with 20 μl of pre-equilibrated anti-FLAG agarose affinity gel (FLAGIPT-1, Sigma-Aldrich) overnight at 4 °C with rotation, washed thrice with CoIP buffer (100 mM NaCl), thrice with wash buffer (50 mM Tris-HCl pH 7.4, 150 mM NaCl) in SigmaPrep spin columns, incubated in 150 μl wash buffer containing 100 μg/ml 3xFLAG peptide for 1 h at 4 °C, and eluted. Samples were analyzed by Western blotting using anti-FLAG M2 (F3165, Sigma-Aldrich) or anti-RNAP β 8RB13 (Thermo Fisher Scientific) monoclonal antibodies. Co-IP results were checked for reproducibility in three independent experiments.

Quantitative chromatin immunoprecipitation (qChIP). Cells grown to exponential phase ($OD_{660} = 0.4–0.6$) in 50 ml M2G-vanillate were cross-linked with 1% final concentration (v/v) formaldehyde for 30 min at room temperature with shaking (100 rpm), quenched with 2.5 ml of 2.1 M glycine, pelleted, washed three times with phosphate-buffered saline, and stored at −80 °C until further use. Cell pellets were resuspended in 200 µl ChIP lysis buffer A (20% sucrose, 50 mM NaCl, 10 mM EDTA, 10 mM Tris pH 8, 1 mg/ml lysozyme), incubated for 30 min at 37 °C and cooled in ice. After mixing with 800 µl ChIP lysis buffer B (150 mM NaCl, 1 mM EDTA, 50 mM HEPES-KOH pH 7.5, 1% Triton X-100, 0.1% deoxycholate, 0.1% SDS, Roche Complete protease inhibitor cocktail), they were sonicated with 12 30s on-30s off cycles in a Bioruptor (Diagenode) to obtain ~0.5 kb long fragments and clarified by centrifugation. 20 µl of the supernatant was kept aside for the input sample. The rest was added to 30 µl of anti-FLAG M2 (F3165, Sigma-Aldrich), anti-σ^A 2G10 (Thermo Fisher Scientific), or anti-RNAP β 8RB13 (Thermo Fisher Scientific) monoclonal antibodies previously immobilized (≥4 h incubation at 4 °C and two washes with PBS containing 5 mg/ml BSA) on protein A magnetic Dynabeads (Life Technologies), and incubated overnight at 4 °C with rotation. The beads were washed twice with ChIP lysis buffer B with 0.15 M NaCl, twice with the same buffer but with 0.5 M NaCl, and twice with wash buffer (250 mM LiCl, 10 mM Tris-HCl pH 8.0, 1 mM EDTA, 0.5% NP-40, 0.5% sodium deoxycholate). After a final wash with Tris-EDTA (TE) buffer, the beads were resuspended in 60 µl TE, 1% SDS, and incubated for 10 min at 65 °C. From this, 40 µl was mixed with 40 µl TE/1% SDS and 2.4 µl proteinase K (20 µg/µl), incubated at 42 °C for 2 h, then at 65 °C for 6 h, and the DNA isolated using the Roche High Pure PCR product Purification kit. The input sample was also subjected to the same cross-link reversal/DNA extraction protocols. qPCR was carried out with SYBR Green reaction mix (BioRad) in 0.1 ml MicroAMP FAST optical 48-well reaction plates and a StepOne qPCR apparatus (Applied Biosystems). Primers used were: 5′-TCCACGGGCGTCTGTTAAG-3′ and 5′-CCCCTCGCGACAATATAACG-3′ for P_{rrnA}; 5′-TGCTCGTGGACGTCAACAAC-3′ and 5′-GGGCGCATAGCCGAGAT-3′ for an intragenic nonpromoter control region (nucleotides 3542858 to 3542913 of gene CCNA_003364, whose σ^F-dependent expression is activated by heavy metal stress[42]). Standard curves were obtained for each DNA region of interest with serially diluted input DNA sample and its primer pair. Signal enrichment at each promoter is the ratio of promoter-specific to intragenic signal of the ChIP fractions relative to that for the input sample, and is reported as the mean and standard error from three independent experiments.

Genome analysis. A database comprising 239 representative complete proteomes of alphaproteobacteria was searched for CdnL homologs using BLASTP and $CdnL_{Cc}$ as a query. Results with an e-value < 0.001 were used for alignments. Protein alignments were performed using MUSCLE v3.8.31[58], and curated with Gblocks 0.91b[59] using default parameters. Phylogenetic trees were generated from the Gblocks output with FastTree version 2.1.7[60] using the Whelan and Goldman amino acid replacement matrix and a Gamma20-based likelihood calculation. The phylogenetic trees were visualized using FigTree v.1.4.2 (http://tree.bio.ed.ac.uk/software/figtree/). 5′ intergenic regions were retrieved from the cognate genomic databases and analyzed independently.

References

1. Lee, D. J., Minchin, S. D. & Busby, S. J. Activating transcription in bacteria. *Annu. Rev. Microbiol.* **66,** 125–152 (2012).
2. Saecker, R. M., Record, M. T. Jr. & deHaseth, P. L. Mechanism of bacterial transcription initiation: RNA polymerase - promoter binding, isomerization to initiation-competent open complexes, and initiation of RNA synthesis. *J. Mol. Biol.* **412,** 754–771 (2011).
3. Ruff, E. F., Record, M. T. & Artsimovitch, I. Initial events in bacterial transcription initiation. *Biomolecules* **5,** 1035–1062 (2015).
4. Abellón-Ruiz, J. *et al.* The CarD/CarG regulatory complex is required for the action of several members of the large set of *Myxococcus xanthus* extracytoplasmic function sigma factors. *Environ. Microbiol.* **16,** 2475–2490 (2014).
5. Cayuela, M. L., Elías-Arnanz, M., Peñalver-Mellado, M., Padmanabhan, S. & Murillo, F. J. The *Stigmatella aurantiaca* homolog of *Myxococcus xanthus* high-mobility-group A-type transcription factor CarD: insights into the functional modules of CarD and their distribution in bacteria. *J. Bacteriol.* **185,** 3527–3537 (2003).
6. García-Heras, F., Padmanabhan, S., Murillo, F. J. & Elías-Arnanz, M. Functional equivalence of HMGA- and histone H1-like domains in a bacterial transcriptional factor. *Proc. Natl. Acad. Sci. USA* **106,** 13546–13551 (2009).
7. Padmanabhan, S., Elías-Arnanz, M., Carpio, E., Aparicio, P. & Murillo, F. J. Domain architecture of a high mobility group A-type bacterial transcriptional factor. *J. Biol. Chem.* **276,** 41566–41575 (2001).
8. Elías-Arnanz, M., Padmanabhan, S. & Murillo, F. J. The regulatory action of the myxobacterial CarD/CarG complex: a bacterial enhanceosome? *FEMS Microbiol. Rev.* **34,** 764–778 (2010).
9. García-Moreno, D. *et al.* CdnL, a member of the large CarD-like family of bacterial proteins, is vital for *Myxococcus xanthus* and differs functionally from the global transcriptional regulator CarD. *Nucleic Acids Res.* **38,** 4586–4598 (2010).
10. Stallings, C. L. *et al.* CarD is an essential regulator of rRNA transcription required for *Mycobacterium tuberculosis* persistence. *Cell* **138,** 146–159 (2009).
11. Yang, X. F. *et al.* Differential expression of a putative CarD-like transcriptional regulator, LtpA, in *Borrelia burgdorferi*. *Infect. Immun.* **76,** 4439–4444 (2008).
12. Kobayashi, K. *et al.* Essential *Bacillus subtilis* genes. *Proc. Natl. Acad. Sci. USA* **100,** 4678–4683 (2003).
13. Rabatinova, A. *et al.* The δ subunit of RNA polymerase is required for rapid changes in gene expression and competitive fitness of the cell. *J. Bacteriol.* **195,** 2603–2611 (2013).
14. Warda, A. K., Tempelaars, M. H., Boekhorst, J., Abee, T. & Nierop Groot, M. N. Identification of CdnL, a putative transcriptional regulator involved in repair and outgrowth of heat-damaged *Bacillus cereus* spores. *PLoS One* **11,** e0148670 (2016).
15. Davis, E., Chen, J., Leon, K., Darst, S. A. & Campbell, E. A. Mycobacterial RNA polymerase forms unstable open promoter complexes that are stabilized by CarD. *Nucleic Acids Res.* **43,** 433–445 (2015).
16. Gallego-García, A. *et al.* Structural insights into RNA polymerase recognition and essential function of *Myxococcus xanthus* CdnL. *PLoS One* **9,** e108946 (2014).
17. Rammohan, J., Ruiz Manzano, A., Garner, A. L., Stallings, C. L. & Galburt, E. A. CarD stabilizes mycobacterial open complexes via a two-tiered kinetic mechanism. *Nucleic Acids Res.* **43,** 3272–3285 (2015).
18. Srivastava, D. B. *et al.* Structure and function of CarD, an essential mycobacterial transcription factor. *Proc. Natl. Acad. Sci. USA* **110,** 12619–12624 (2013).
19. Bae, B. *et al.* CarD uses a minor groove wedge mechanism to stabilize the RNA polymerase open promoter complex. *Elife* **4,** e08505 (2015).

20. Bernal-Bernal, D. *et al.* Structure-function dissection of *Myxococcus xanthus* CarD N-terminal domain, a defining member of the CarD_CdnL_TRCF family of RNA polymerase interacting proteins. *PLoS One* **10,** e0121322 (2015).
21. Weiss, L. A. *et al.* Interaction of CarD with RNA polymerase mediates *Mycobacterium tuberculosis* viability, rifampin resistance, and pathogenesis. *J. Bacteriol.* **194,** 5621–5631 (2012).
22. Gallego-García, A., Mirassou, Y., Elías-Arnanz, M., Padmanabhan, S. & Jiménez, M. A. NMR structure note: N-terminal domain of *Thermus thermophilus* CdnL. *J. Biomol. NMR* **53,** 355–363 (2012).
23. Ryan, K. R. & Shapiro, L. Temporal and spatial regulation in prokaryotic cell cycle progression and development. *Annu. Rev. Biochem.* **72,** 367–394 (2003).
24. Williams, K. P., Sobral, B. W. & Dickerman, A. W. A robust species tree for the alphaproteobacteria. *J. Bacteriol.* **189,** 4578–4586 (2007).
25. Zhou, B. *et al.* The global regulatory architecture of transcription during the *Caulobacter* cell cycle. *PLoS Genet.* **11,** e1004831 (2015).
26. Malakooti, J., Wang, S. P. & Ely, B. A consensus promoter sequence for *Caulobacter crescentus* genes involved in biosynthetic and housekeeping functions. *J. Bacteriol.* **177,** 4372–4376 (1995).
27. Thanbichler, M., Iniesta, A. A. & Shapiro, L. A comprehensive set of plasmids for vanillate- and xylose-inducible gene expression in *Caulobacter crescentus*. *Nucleic Acids Res.* **35,** e137 (2007).
28. Schluter, J. P. *et al.* Global mapping of transcription start sites and promoter motifs in the symbiotic α-proteobacterium *Sinorhizobium meliloti* 1021. *BMC Genom.* **14,** 156 (2013).
29. Christen, B. *et al.* The essential genome of a bacterium. *Mol. Syst. Biol.* **7,** 528 (2011).
30. Curtis, P. D. & Brun, Y. V. Identification of essential alphaproteobacterial genes reveals operational variability in conserved developmental and cell cycle systems. *Mol. Microbiol.* **93,** 713–735 (2014).
31. Pechter, K. B., Gallagher, L., Pyles, H., Manoil, C. S. & Harwood, C. S. Essential genome of the metabolically versatile alphaproteobacterium *Rhodopseudomonas palustris*. *J. Bacteriol.* **198,** 867–876 (2015).
32. Perry, B. J., Akter, M. S. & Yost, C. K. The use of transposon insertion sequencing to interrogate the core functional genome of the legume symbiont *Rhizobium leguminosarum*. *Front. Microbiol.* **7,** 1873 (2016).
33. Bhat, N. H., Vass, R. H., Stoddard, P. R., Shin, D. K. & Chien, P. Identification of ClpP substrates in *Caulobacter crescentus* reveals a role for regulated proteolysis in bacterial development. *Mol. Microbiol.* **88,** 1083–1092 (2013).
34. Jenal, U. & Fuchs, T. An essential protease involved in bacterial cell-cycle control. *EMBO J* **17,** 5658–5669 (1998).
35. Williams, B., Bhat, N., Chien, P. & Shapiro, L. ClpXP and ClpAP proteolytic activity on divisome substrates is differentially regulated following the *Caulobacter* asymmetric cell division. *Mol. Microbiol.* **93,** 853–866 (2014).
36. Potocka, I., Thein, M., Østerås, M., Jenal, U. & Alley, M. R. Degradation of a *Caulobacter* soluble cytoplasmic chemoreceptor is ClpX dependent. *J. Bacteriol.* **184,** 6635–6641 (2002).
37. Chien, P., Perchuk, B. S., Laub, M. T., Sauer, R. T. & Baker, T. A. Direct and adaptor-mediated substrate recognition by an essential AAA+ protease. *Proc. Natl. Acad. Sci. USA* **104,** 6590–6595 (2007).
38. Domian, I. J., Quon, K. C. & Shapiro, L. Cell type-specific phosphorylation and proteolysis of a transcriptional regulator controls the G1-to-S transition in a bacterial cell cycle. *Cell* **90,** 415–424 (1997).
39. Gulten, G. & Sacchettini, J. C. Structure of the *Mtb* CarD/RNAP β-lobes complex reveals the molecular basis of interaction and presents a distinct DNA-binding domain for *Mtb* CarD. *Structure* **21,** 1859–1869 (2013).
40. Kaur, G., Dutta, D. & Thakur, K. G. Crystal structure of *Mycobacterium tuberculosis* CarD, an essential RNA polymerase binding protein, reveals a quasidomain-swapped dimeric structural architecture. *Proteins* **82,** 879–884 (2014).
41. Haakonsen, D. L., Yuan, A. H. & Laub, M. T. The bacterial cell cycle regulator GcrA is a σ^{70} cofactor that drives gene expression from a subset of methylated promoters. *Genes Dev.* **29,** 2272–2286 (2015).
42. Kohler, C., Lourenco, R. F., Avelar, G. M. & Gomes, S. L. Extracytoplasmic function (ECF) sigma factor σ^{E} is involved in *Caulobacter crescentus* response to heavy metal stress. *BMC Microbiol.* **12,** 210 (2012).
43. Boutte, C. C. & Crosson, S. The complex logic of stringent response regulation in *Caulobacter crescentus*: starvation signalling in an oligotrophic environment. *Mol. Microbiol.* **80,** 695–714 (2011).
44. Garner, A. L., Weiss, L. A., Manzano, A. R., Galburt, E. A. & Stallings, C. L. CarD integrates three functional modules to promote efficient transcription, antibiotic tolerance, and pathogenesis in mycobacteria. *Mol. Microbiol.* **93,** 682–697 (2014).
45. Keiler, K. C. & Shapiro, L. TmRNA is required for correct timing of DNA replication in *Caulobacter crescentus*. *J. Bacteriol.* **185,** 573–580 (2003).
46. Murray, S. M., Panis, G., Fumeaux, C., Viollier, P. H. & Howard, M. Computational and genetic reduction of a cell cycle to its simplest, primordial components. *PLoS Biol.* **11,** e1001749 (2013).
47. Gonzalez, D. & Collier, J. DNA methylation by CcrM activates the transcription of two genes required for the division of *Caulobacter crescentus*. *Mol. Microbiol.* **88,** 203–218 (2013).
48. Budde, I., Steil, L., Scharf, C., Volker, U. & Bremer, E. Adaptation of *Bacillus subtilis* to growth at low temperature: a combined transcriptomic and proteomic appraisal. *Microbiology* **152,** 831–853 (2006).
49. Barnett, M. J., Bittner, A. N., Toman, C. J., Oke, V. & Long, S. R. Dual RpoH sigma factors and transcriptional plasticity in a symbiotic bacterium. *J. Bacteriol.* **194,** 4983–4994 (2012).
50. Blanc, G. *et al.* Reductive genome evolution from the mother of Rickettsia. *PLoS Genet.* **3,** e14 (2007).
51. Raju, R. M. *et al.* Post-translational regulation via Clp protease is critical for survival of *Mycobacterium tuberculosis*. *PLoS Pathog* **10,** e1003994 (2014).
52. Flynn, J. M., Neher, S. B., Kim, Y. I., Sauer, R. T. & Baker, T. A. Proteomic discovery of cellular substrates of the ClpXP protease reveals five classes of ClpX-recognition signals. *Mol. Cell* **11,** 671–683 (2003).
53. Chandrangsu, P., Lemke, J. J. & Gourse, R. L. The *dksA* promoter is negatively feedback regulated by DksA and ppGpp. *Mol. Microbiol.* **80,** 1337–1348 (2011).
54. Whipple, F. W. & Sonenshein, A. L. Mechanism of initiation of transcription by *Bacillus subtilis* RNA polymerase at several promoters. *J. Mol. Biol.* **223,** 399–414 (1992).
55. Karimova, G., Ullmann, A. & Ladant, D. A bacterial two-hybrid system that exploits a cAMP signaling cascade in *Escherichia coli*. *Methods Enzymol.* **328,** 59–73 (2000).
56. García-Heras, F., Abellón-Ruiz, J., Murillo, F. J., Padmanabhan, S. & Elías-Arnanz, M. High-mobility-group A-like CarD binds to a DNA site optimized for affinity and position and to RNA polymerase to regulate a light-inducible promoter in *Myxococcus xanthus*. *J. Bacteriol.* **195,** 378–388 (2013).
57. López-Rubio, J. J. *et al.* Operator design and mechanism for CarA repressor-mediated down-regulation of the photoinducible *carB* operon in *Myxococcus xanthus*. *J. Biol. Chem.* **279,** 28945–28953 (2004).
58. Edgar, R. C. MUSCLE: multiple sequence alignment with high accuracy and high throughput. *Nucleic Acids Res.* **32,** 1792–1797 (2004).
59. Talavera, G. & Castresana, J. Improvement of phylogenies after removing divergent and ambiguously aligned blocks from protein sequence alignments. *Syst. Biol.* **56,** 564–577 (2007).
60. Price, M. N., Dehal, P. S. & Arkin, A. P. FastTree 2-approximately maximum-likelihood trees for large alignments. *PLoS One* **5,** e9490 (2010).

Acknowledgements

We thank José Antonio Madrid and Victoria López Egea (Universidad de Murcia) for technical assistance. We thank Prof. Lucy Shapiro (Stanford University) for providing anti-CtrA antibodies. This work was funded by grants BFU2012-40184-C02-01 and BFU2015-67968-C2-1-P from the Spanish Ministerio de Economía y Competitividad (MINECO) and co-financed with FEDER funds, 19429/PI/14 from Fundación Séneca (Agencia de Ciencia y Tecnología, Región de Murcia, Spain) to M.E.-A., BFU2012-40184-C02-02 and BFU2015-67968-C2-2-P from MINECO to S.P., a Ph.D. fellowship from MINECO to A.G.-G., and grant 31003A_140758 from the Swiss National Science Foundation to J.C.

Author Contributions

A.G.-G., A.A.I., D.G., J.C., S.P. and M.E.-A. conceived and designed experiments. A.G.-G., A.A.I., D.G. and M.E.-A. performed the experiments. A.G.-G., A.A.I., D.G., J.C., S.P. and M.E.-A. analysed data. D.G., A.A.I., J.C. and M.E.-A. contributed reagents/materials/analysis tools. S.P. and M.E.-A. wrote the manuscript, with contribution from all other authors. All authors read and approved the final manuscript.

Additional Information

Supplementary information accompanies this paper at http://www.nature.com/srep

Competing financial interests: The authors declare no competing financial interests.

How to cite this article: Gallego-García, A. *et al. Caulobacter crescentus* CdnL is a non-essential RNA polymerase-binding protein whose depletion impairs normal growth and rRNA transcription. *Sci. Rep.* **7**, 43240; doi: 10.1038/srep43240 (2017).

Publisher's note: Springer Nature remains neutral with regard to jurisdictional claims in published maps and institutional affiliations.